ALPHA DECAY

OF EXCITED STATES OF CARBON-12

D. SHACKLETON

A thesis written in partial fulfilment of the requirements

for the degree of Master of Science at the

University of Cape Town.

October, 1970.

ABSTRACT

A crystal of the carbon-rich phosphor, anthracene, has been bombarded by monoenergetic fast neutrons. Alpha-particle decays of carbon nuclei have been separated from other events by a specialised application of the pulse shape discrimination technique. A numerical analysis of the data has yielded alpha-particle energy spectra over a wide energy range.

A counter has been assembled to detect neutrons scattered by carbon nuclei in the crystal, and the measurements repeated in coincidence with these neutrons. The energy range of particle resolving power has been extended. Structure in the resulting alpha-particle and proton energy spectra is attributed to particle decays of specific levels in carbon-12. It is shown how the experiment may be modified and extended to measure decay parameters in absolute terms.

****

TABLE OF CONTENTS

CHAPTER 1

INTRODUCTION

1.1 ALPHA DECAY STUDIES

Particle decays of excited states of the carbon-12 nucleus have been studied by several experimenters in recent years. Many different approaches have been adopted for populating levels in this nucleus. For a comprehensive survey the reader is referred to the compilation of energy level data by Ajzenberg-Selove and Lauritsen (1968).

Of particular relevance to the present study are experiments utilising inelastic neutron scattering on the nucleus of interest to provide the primary excitation. Nuclear emulsion studies have provided useful information on the channels used by the decays of the first few states of carbon-12 (see Perkin 1951, Frye et al. 1955). Here neutron bombardment of a film of carbon-rich emulsion was used to raise carbon-12 nuclei to excited levels. Charged particle decays produced visible tracks whose range and direction permitted identification of the nuclear reactions involved. Cases where the final state included three independent alpha-particles were identified by the formation of three-pronged "stars".

Inelastic scattering of neutrons from graphite has been used in conjunction with a neutron time of flight spectrometer by Barjon et al. (1962) and others, to yield differential inelastic scattering cross sections corresponding to individual final states of the recoiling carbon nuclei. Barjon's measurements were made for a primary neutron energy of 15 MeV; an interesting contribution was

found in the time of flight spectrum which could not be connected with levels in carbon, and it was attributed to the reaction, $^{12}C(n,\alpha)^{9}Be^{*}(n)^{8}Be$, with the intermediate beryllium-9 nucleus being excited to a level at 6.76 MeV.

A comprehensive study at 14.1 MeV has been undertaken by Joseph et al. (1967) using the same technique; these experimenters measured detailed angular distributions corresponding to the carbon-12 levels at 4.43, 7.65 and 9.63 MeV, correcting their results for multiple scattering in the sample by a Monte Carlo calculation, and using maximum likelihood theory to estimate errors due to background subtraction. Joseph et al. found a broad neutron group which could not be explained by inelastic scattering from carbon. It was suggested that this group was due to inelastic scattering from a broad level in carbon at about 10.1 MeV, in addition to various sequential decays of which the (n,α) reaction was the first step.

The existence of this broad level was suggested by Peelle (1957) on the strength of results from inelastic scattering of 16.7 MeV protons from carbon. Confirmation of the excitation of carbon nuclei to this level has been sought by Grin et al. (1965, 1966, 1969) and others, but its existence still seems to be in doubt.

A new approach to particle decay studies of carbon-12 states has become possible with the advent of pulse shape discrimination systems used with organic scintillation detectors (Brooks 1956,

Owen 1958). Johnson (1963) has used a single scintillation counter to observe alpha-particles arising from the bombardment of a stilbene crystal by 14.85 MeV neutrons.

Grin et al. (1965) have devised an ingenious experiment, extending the neutron time-of-flight technique for use with organic scintillators equipped with pulse shape discrimination circuitry. The experiment involved neutron bombardment of a plastic scintillator, and permitted recording of differential cross sections for inelastic scattering from carbon nuclei for the first three excited states; some idea could also be gained of the branching ratios for electromagnetic and alpha-particle decays of these states by amplitude discrimination. Again, the neutron energy was 14.1 MeV.

The following section outlines the approach of Johnson (1963), as extended for the requirements of the present investigation, and briefly describes those properties of organic phosphors which make the approach possible.

1.2 ORGANIC PHOSPHORS

Phosphors find application in nuclear physics as charged particle detectors and, indirectly, as detectors of other ionising radiations which give rise to charged particles or ions, by reaction or scattering processes within the phosphor. In particular, in a study of properties of carbon nuclei, a carbon-rich phosphor may be used as both target and detector. Fast neutrons incident on a phosphor populate certain excited states of carbon nuclei

by inelastic scattering; a decay proceeding by charged particle emission produces a scintillation in the phosphor which may be amplified by means of a photomultiplier tube.

In the present study a crystal of anthracene is irradiated with monoenergetic fast neutrons; ideally it is desired to record only those scintillations induced by alpha-particles. There are two major sources of background signal to contend with. Many incident neutrons do not interact with carbon nuclei but are instead scattered by hydrogen nuclei within the phosphor, the recoil protons producing scintillations. Also there is a high flux of background gamma radiation produced by neutron interaction with surrounding materials, as well as by electromagnetic decays of carbon states within the phosphor itself, giving rise to electron-induced scintillations from gamma-ray-electron interactions.

It has been known for some time that in certain phosphors, a particle-induced scintillation is composed of an intense fast decaying and a slowly decaying component, so that the light output may be approximated by

$$L = Ae^{-t/\tau_1} + Be^{-t/\tau_2}, \qquad \tau_2 \gg \tau_1 .$$

For the crystalline organic phosphor anthracene, Owen (see Birks, 1964) has determined $\tau_1 \doteq 33$ns and $\tau_2 \doteq 370$ns. The importance of this lies in the fact that the ratio B/A is dependent on the energy loss of the ionising particle per unit distance, dE/dx, which is in turn determined by the nature of the particle.

In anthracene B/A for a proton is given by Birks (1964) as approximately twice that for an electron. An alpha-particle induces an even higher slow to fast component ratio. This property has been taken advantage of by Brooks (1956, 1959), Owen (1958) and others, who have operated a photomultiplier tube with a low potential difference between the last dynode and the anode, so that an amplified pulse produces space-charge saturation in this region. In the Brooks circuit, a simple passive network mixes the outputs from the last dynode and the anode. The mixed output has greater amplitude if induced by a recoiling proton than if arising from an electron recoil, for equivalent integrated light outputs of the phosphor. Full details of the theory of operation of this circuit have been described by Brooks (1959).

This pulse shape discrimination (PSD) technique has been successfully applied to liquid scintillators too. For the liquid scintillator NE213 Henchoz (1965) has found $\tau_1 \doteq 2.5$ns and $\tau_2 \doteq 150$ns, with B/A $\doteq 0.7\%$ for electrons and $\doteq 1.4\%$ for protons.

There is an additional scintillation property, however, applicable only to crystalline phosphors; it is an assymetry effect associated with the crystal axes. For anthracene, stilbene and certain other qrystals, Tsukada and Kikuchi (1962) and others have shown that the height and shape of a scintillation pulse each depend on the direction of the particle trajectory with respect to the crystal axes. In the present study an anthracene crystal was placed at the optimum orientation (found by experiment) with

respect to a fast neutron beam for pulse shape discrimination outputs deriving from proton- and alpha- induced crystal excitations to be as markedly separated as possible.

The Brooks and Owen PSD circuits have been criticised on two accounts. Batchelor et al. (1960) have pointed out that the circuits producing the pulse shape discrimination signal do not remove the possible overshoot produced when the pulse returns to zero voltage. Detection of overshoots is obviated in the present investigation by the use of a gating circuit, described in Chapter 2.

de Vries and Udo (1961) have found it necessary to introduce an interference network into the Owen circuit to reject pile-up effects encountered in experiments involving high count rate. As the highest detected scintillation rate was 9.4 kHz in the present study, no such modification was required.

The initial energy of an electron in anthracene is proportional to the response (luminous intensity) produced in this phosphor. This holds true over an appreciable energy range. For heavier charged particles and ions, however, the relationship is not a linear one. Brooks (see Birks, 1964) has obtained these relationships for electrons, protons and alpha particles (see figure 1.2). Gooding and Pugh (1960) have suggested a design for a linear scintillation counter; no attempt has been made to construct such a counter for this work, and the curves of figure 1.2 have been used for quantitative calibrations.

Carbon nuclei were bombarded with neutrons of energy as great as 22 MeV in this investigation; figure 1.1 shows those excited

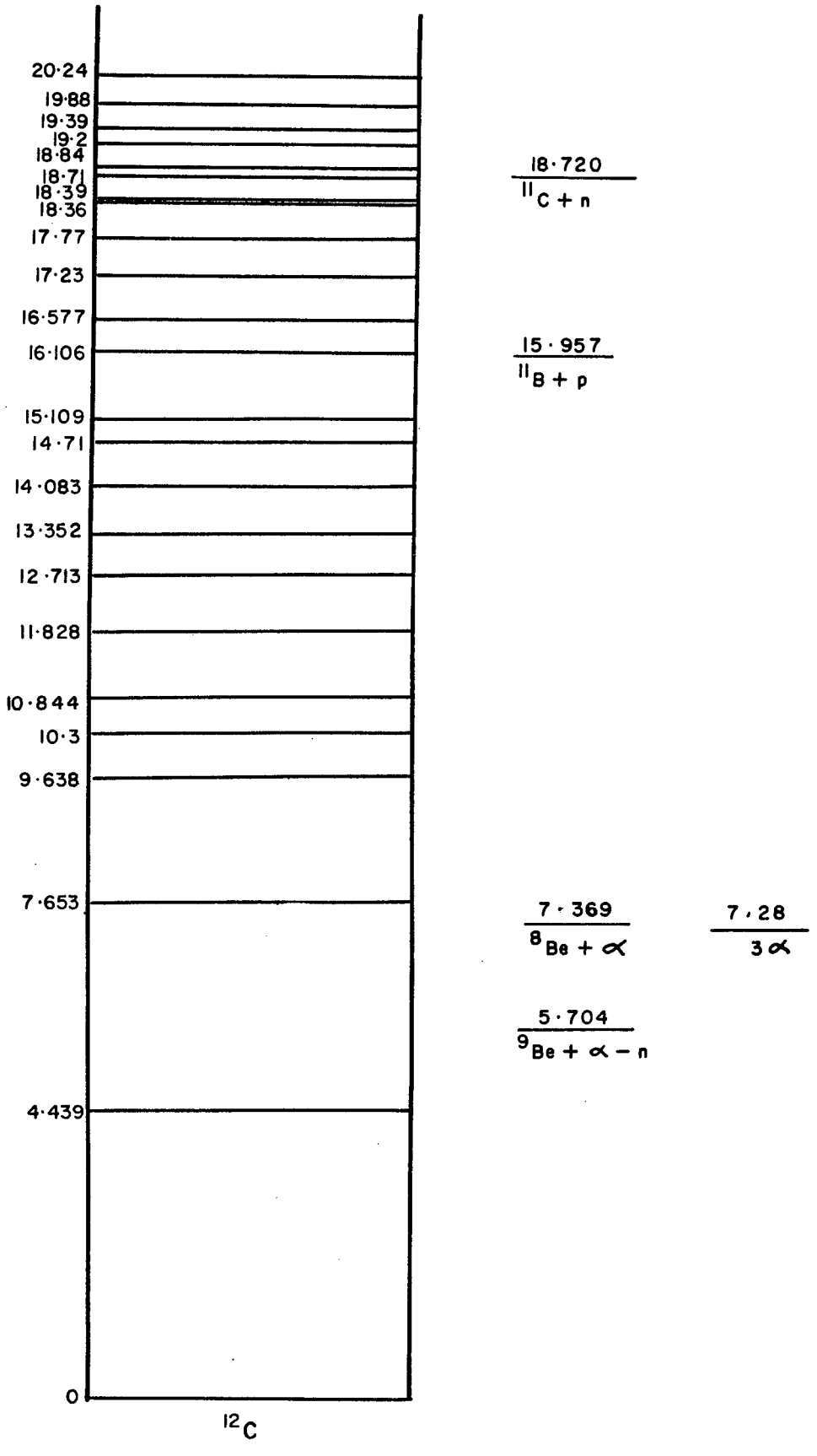

Fig. 1.1 Energy levels of Carbon − 12, in MeV.

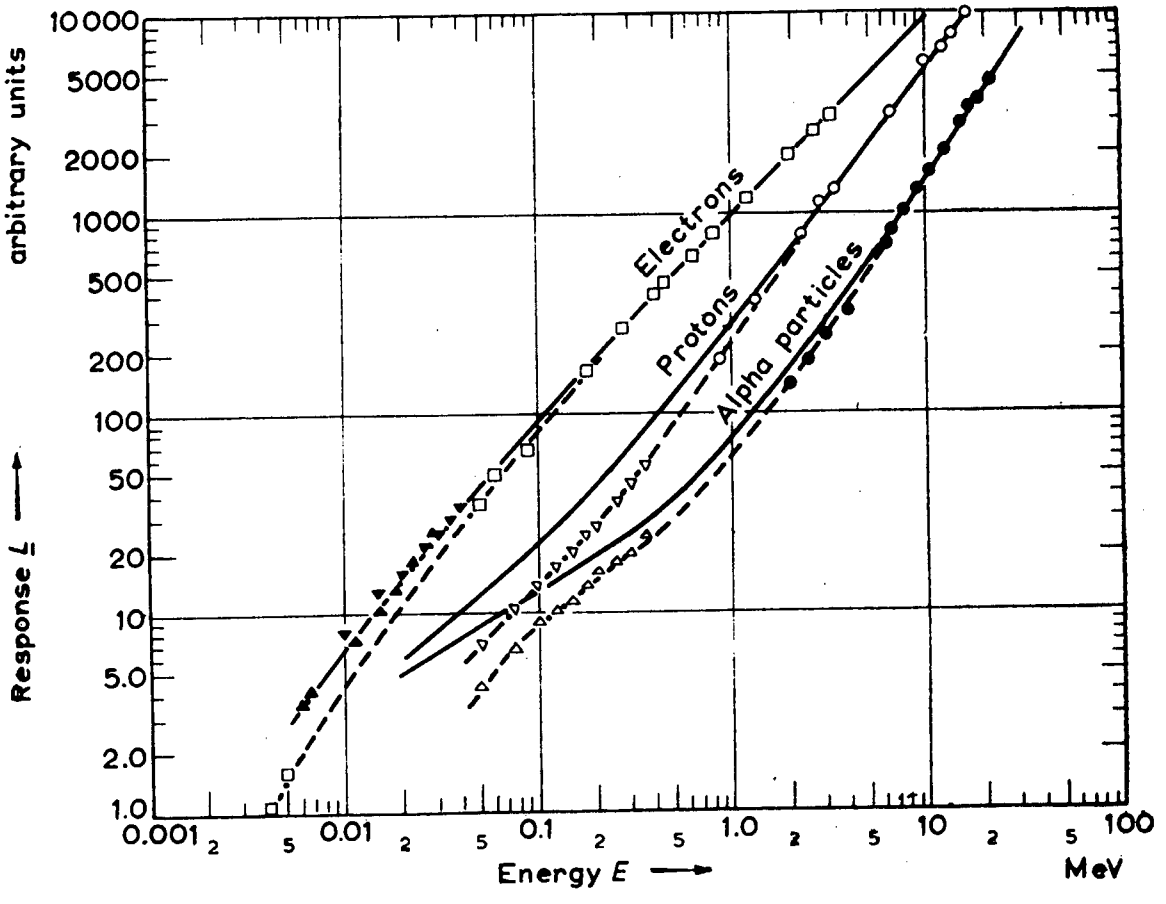

Fig. I.2 Response of an anthracene crystal to electrons, protons and alpha - particles.

---- external radiation , measured.

——— internally generated radiation, calculated.

states which can be populated by neutrons of this energy (taken from Ajzenberg-Selove and Lauritsen, 1968).

While pulse shape discrimination may be applied to separate alpha-particle events from proton and electron recoil contributions, there will inevitably be a contaminating background of alpha-particles from the reaction $^{12}C(n,\alpha)^{9}Be(g.s.)$, a process which sheds no light on decay of carbon-12 states.

1.3 OBJECTS OF THE PRESENT INVESTIGATION

The primary aims of the present study are to use the compact target-cum-detector approach to investigate the disintegration by alpha-particle emission of carbon-12 nuclei; also to study reactions arising from fast neutron bombardment of the organic hydrocarbon phosphor, anthracene. Furthermore it is intended to seek indications of the existence of an energy level at 10.1 MeV in carbon-12, searched for by Johnson (1963), Joseph (1967), Grin (1969) and others, and peculiar in that the width of this level appears to be some 2 MeV. It is also proposed to extend the effective resolution of proton and alpha-particle events in a scintillation counter down to low energies. Finally, in order to make comparisons with the results of previous authors, branching ratios for decay channels of individual states are to be sought; this requires additional information specifying the rates of population of states under fast neutron bombardment, for which purpose differential inelastic scattering cross-sections are to be measured using a neutron time of flight technique.

CHAPTER 2

EXPERIMENTAL ARRANGEMENTS

Detailed descriptions of apparatus used in this project are given in this Chapter for the three major experiments performed. Much preliminary laboratory work was carried out to study the variables in the Brooks PSD circuit and auxiliary electronic equipment, using radioactive sources, so that optimum discrimination conditions could be achieved; also timing resolution of a few nanoseconds was sought after.

Altogether four detectors were used. It was judged that the best pulse shape discrimination conditions for the present application were obtained with an EMI 6097 photomultiplier tube, and this was used where no timing measurements were necessary. A timing resolution of 3ns was obtained for two RCA 6810A tubes (used with a Chronetics model 151 "leading-edge" discriminator), one equipped with a PSD circuit and the other arranged to give a fast anode output and a linear 5th dynode output only. The fourth detector used in this project was built by Jones (1967) and used a Philips 58 AVP tube to provide 3ns timing resolution and γ-n discrimination.

2.1 NEUTRON PRODUCTION

In each of the experimental arrangements described below, a source of monoenergetic fast neutrons was obtained from the reaction $^{3}H(d,n)^{4}He$, with the primary deuterons generated as a collimated monoenergetic beam by the S.U.N.I. 5.5 MV Van der Graaff

accelerator. A tritium gas cell was used as the target for preliminary work; a tritium target consisting of one Curie of tritium adsorbed onto titanium on a gold backing was subsequently obtained and used for all measurements. This target was subjected to up to 3 microamperes of deuteron current at 5 MeV, and it was accordingly necessary to apply a cooling system to it.

A liquid nitrogen cold trap was coupled to the target by means of a stainless steel cold finger. A thermocouple was situated inside the cold trap at about half the maximum liquid nitrogen level. Whenever its temperature rose appreciably above the boiling point of nitrogen, this thermocouple activated a pumping mechanism which automatically refilled the trap. A chart recorder situated in the control area was used to monitor the temperature of this thermocouple. As a safety precaution, a second thermocouple was situated somewhat lower in the trap, and used to trigger an alarm bell.

The "solid" target had two distinct advantages over the gas cell, in addition to greater ease of handling. Firstly, the location of the neutron source was now accurately defined. Secondly, no window was required to separate the tritium from the high vacuum of the accelerator tube, and consequently a major source of deuteron energy reduction and spread was removed.

2.2 NEUTRON DETECTION

A crystal of anthracene was optically coupled to the face of a type EMI 6097 photomultiplier tube by a film of liquid paraffin. The size of this crystal was approximately 1.5 cm^3. The crystal surfaces not in contact with the photomultiplier were covered with a thin, reflecting aluminium foil to improve the efficiency of light-collection. This assembly was enclosed in an aluminium housing, held by a support which, while keeping the crystal and the axis of the photomultiplier tube in the horizontal plane defined by the target, permitted rotations of the detector about the vertical axis through the crystal (angle θ) and about the axis of the photomultiplier tube (angle ϕ). Provision was also made for rotation of the whole combination about a vertical axis through the tritium target (angle γ). These angles are represented in figure 2.1. The incident neutron energy could thus be selected by appropriate choice of angle γ, while any axis through the crystal could be aligned with the incident neutron direction by variation of angles θ and ϕ. A boron "long-counter" which viewed the neutron source directly was set up as a neutron monitor. This counter comprised a BF_3 detector surrounded by a cylindrical paraffin wax modulator.

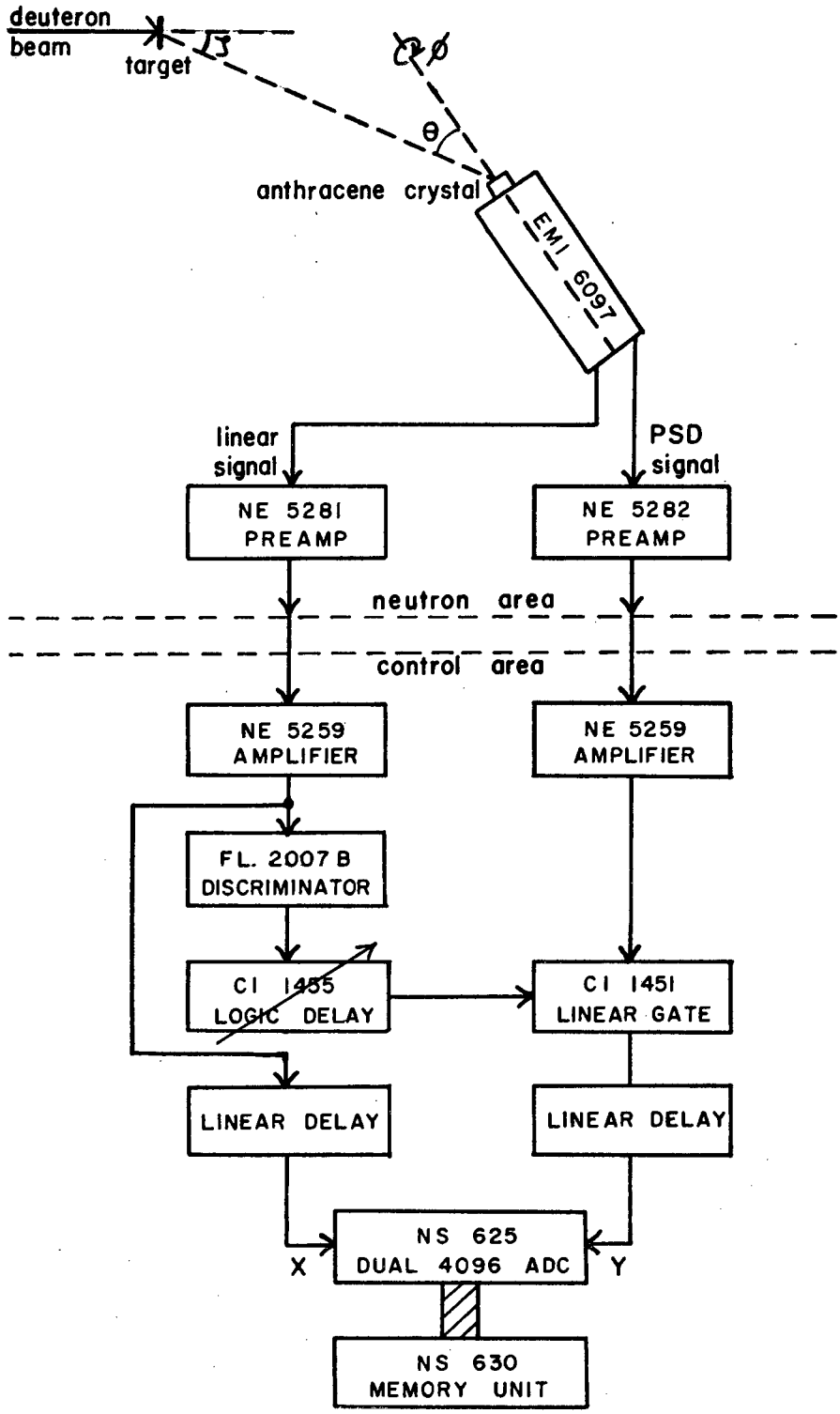

Fig. 2.1 Block diagram illustrating angles γ, θ and ϕ, and showing circuit used to select time of observation of PSD signal for two-parameter analysis.

2.3 PULSE SHAPE DISCRIMINATION SYSTEM

A pulse shape discrimination circuit of the type developed by Brooks (1956, 1959) and described previously in Section 1.2 was mounted within the aluminium detector housing (see figure 2.2).

The output pulses from the PSD amplifier for excitations due to electrons, protons and alpha particles differ in amplitude most significantly at some time t after the initial rise, and a circuit was used to interrogate the PSD output at this time (see figure 2.1), producing a "gated PSD" signal. The width of the gating signal was limited to reject overshoots (Batchelor et al., 1960).

In the present study the PSD technique of particle identification has found two distinct applications. The simpler of these is the now conventional application, where an amplitude discriminator is applied to the gated PSD signal and adjusted to produce a logic pulse if a neutron was detected, but no pulse in the case of an incident gamma ray. This application is used to convert a standard scintillation counter into a neutron counter, and is employed in the present investigation as the detector in a neutron time of flight spectrometer (see Section 2.5 and Chapter 4).

Pulse shape discrimination has been used here in another way. The technique has been applied not only to eliminate gamma ray background, but to distinguish alpha-particle events from proton events.

The amplitude of the PSD signal from the photomultiplier tube is dependent both on pulse height and pulse shape, and therefore

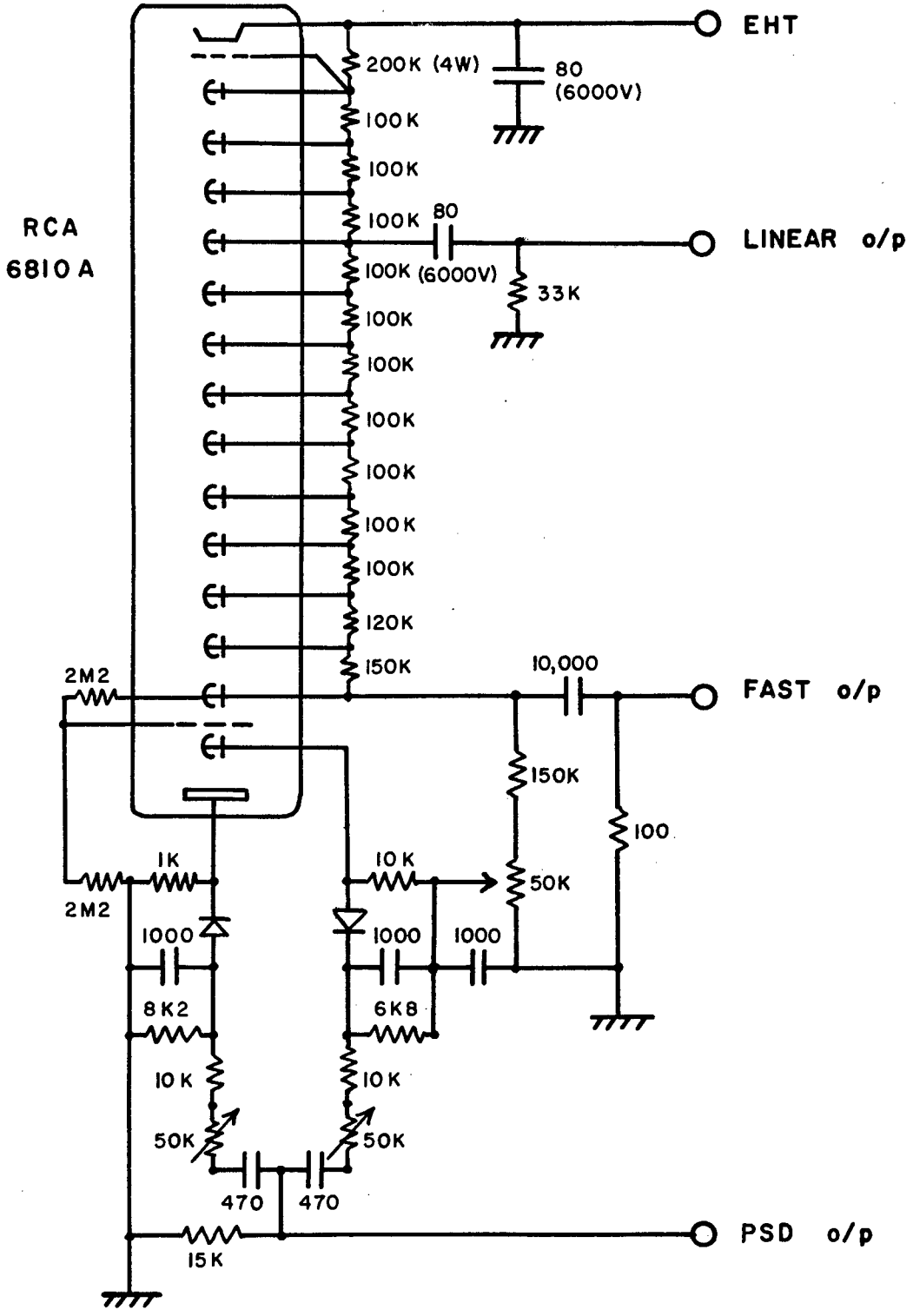

Fig. 2.2 Pulse shape discrimination system used with an RCA 6810 A photomultiplier tube, the whole being enclosed in the detector housing.

on the energy as well as the nature of the exciting particle. We may therefore construct a plot of the amplitude of the gated PSD signal as a function of energy, and we will obtain one curve for each type of particle considered. In the present experiment this process has been carried out electronically, in that the linear and gated PSD signals were aligned in time using suitable microsecond delays, and fed to the X and Y inputs of a Northern Scientific dual parameter analog to digital converter. (See figure 2.1). The two parameter digital information generated by each scintillation was recorded in a Northern Scientific 12-bit Memory Unit, the 4096-channel capacity of this unit being utilized as 128 channels for linear pulse amplitude and 32 channels for the gated PSD pulse amplitude. The contents of the Memory Unit could be displayed by a built-in oscilloscope in contour and isometric formats. Figure 2.2A has been traced from a photograph of the contour mode oscilloscope readout, and demonstrates the dependence of the gated PSD signal on both energy and particle type. The data were also punched onto computer cards (automatically in some cases) and printed out by a parallel printer.

It was necessary to calibrate the energy axis of the 32 x 128 element matrix of channels, and this was performed as follows. The detector was exposed to gamma-rays from a cobalt-60 source in place of fast neutrons, and a 2-parameter spectrum was recorded with the PSD amplifier gain boosted so that the electron-recoil locus occupied a prominent region of the matrix. The gain of

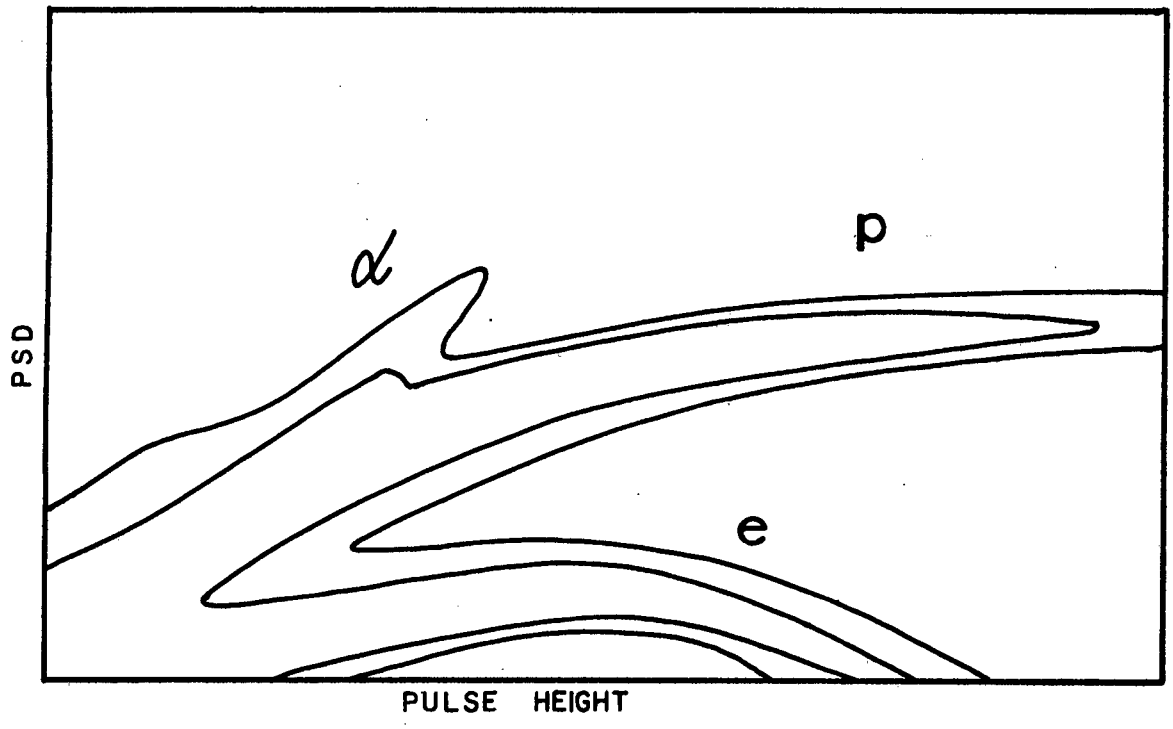

Fig. 2.2A Pulse shape discrimination amplitude as a function of energy and particle type.

the linear signal amplifier was then increased by a factor of 2.5 and a second spectrum superimposed on the first. (See figure 2.3.)

Integrations over PSD channel number in the region of the first locus yielded the characteristic electron energy spectrum induced by Co-60 gamma rays; the Compton "edge" of the highest energy is attributed to 1.33 MeV gamma rays, and the position of this edge in the spectrum therefore corresponds to an electron energy equal to the maximum recoil energy attained by a Compton recoil electron from a 1.33 MeV gamma ray, viz. 1.12 MeV. A comparison of the two loci indicates the channel of zero pulse height. The axis is now calibrated in terms of electron energy, and hence also proton and alpha energies, from the response curves for anthracene (see figure 1.2).

Experiments carried out with this system, together with the results obtained, are described in Chapter 3.

2.4 COINCIDENCE SYSTEM

While the alpha and proton loci obtained with the dual parameter system described above are well resolved at high energy, the separation becomes less clearly defined in the region of low light output (discussed in Chapter 3). In view of this an extension of the above experimental system was devised in order to suppress the recording of n-p scattering data.

The EMI 6097 tube was replaced by an RCA 6810 A tube. The wiring of these two tubes was essentially the same. A second

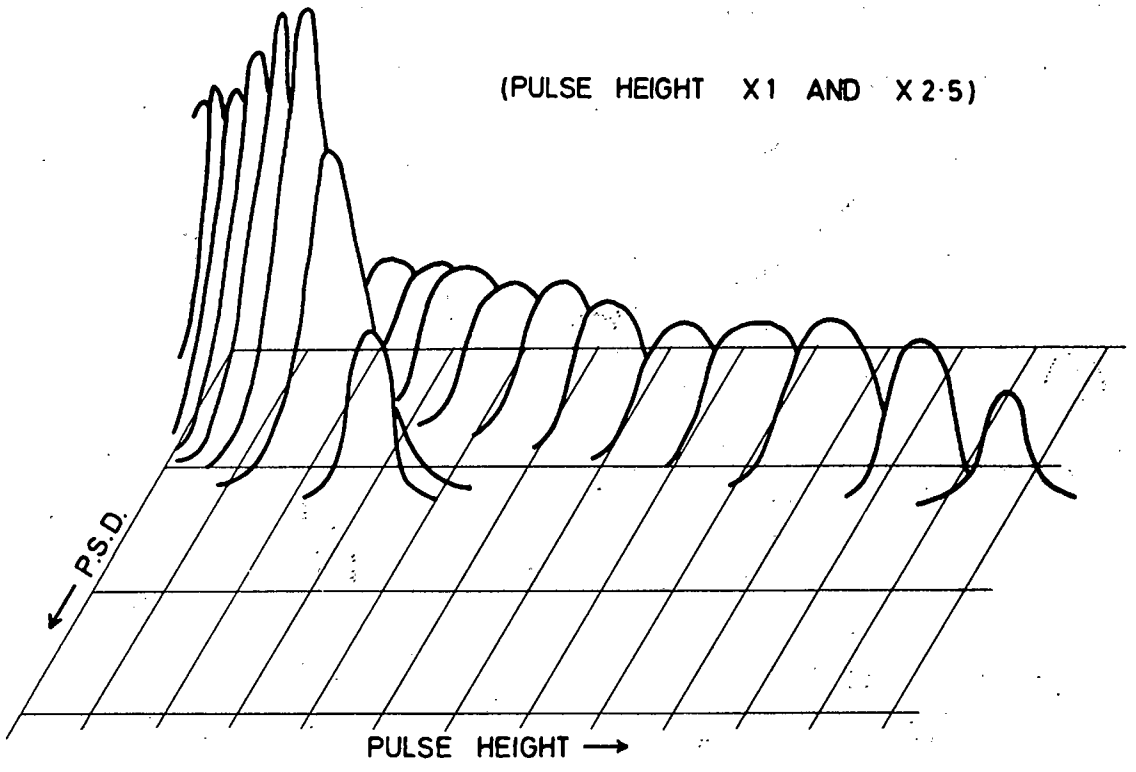

Fig. 2.3 Loci due to Co-60 gamma rays.

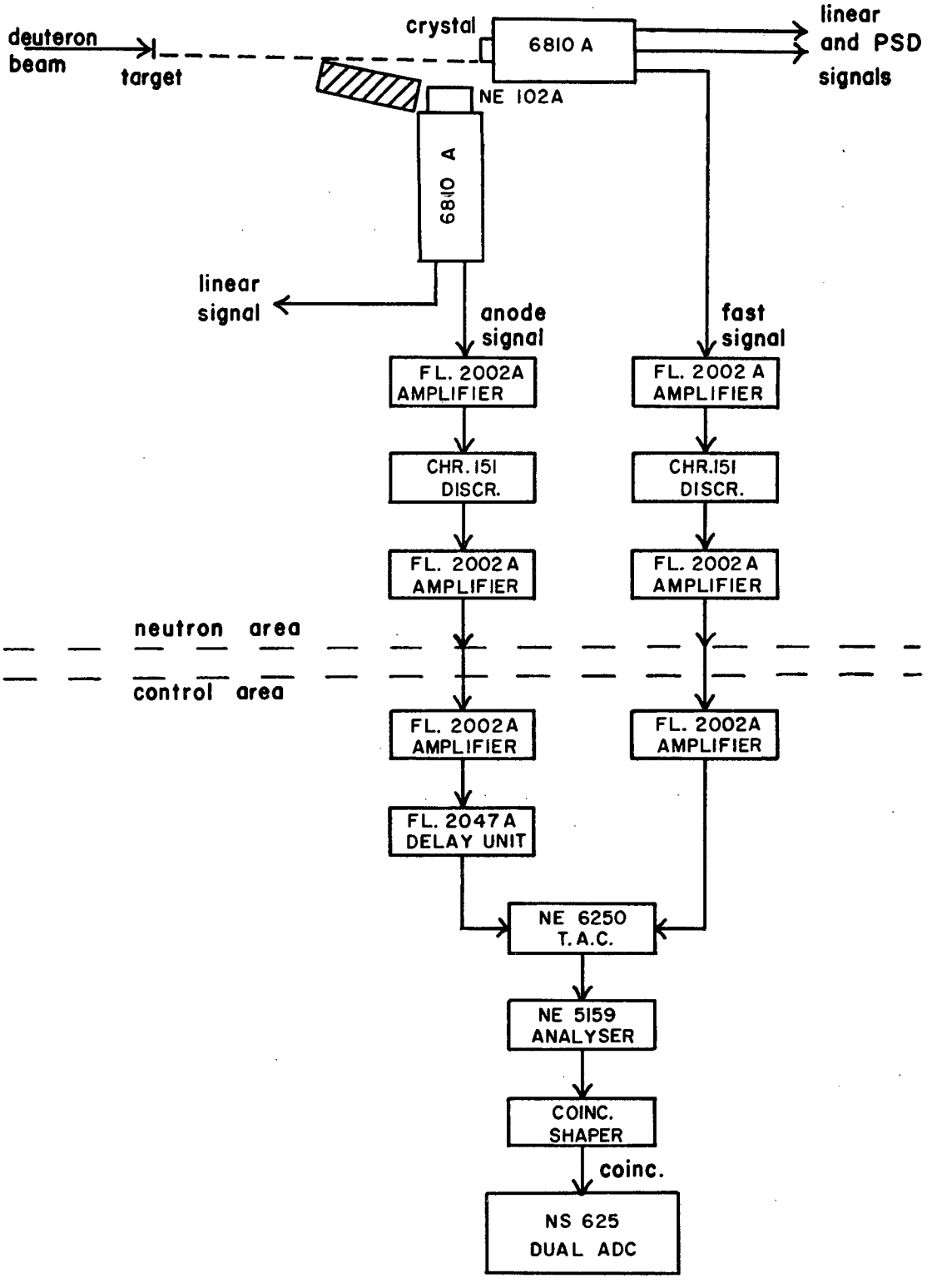

Fig. 2.4 Fast coincidence arrangement for suppression of n–p scattering data acquisition. The circuit forms an auxiliary to that of figure 2.1.

The circuit of figure 2.4 was used to generate a fast coincidence signal when a scintillation occurred in the plastic phosphor within approximately 10 ns of a scintillation in the anthracene crystal. Linear and gated PSD pulse heights originating in the crystal were recorded only for those events in coincidence with this signal.

Data were accumulated in sets each consisting of three experimental runs. The first run used the coincidence arrangement described above to record true coincidences. For the second run the 10 ns acceptable range of neutron flight times was deliberately misaligned to record random coincidences. In the third run the coincidence requirement was removed (switch-selectable on the dual ADC) and two parameter information was stored whether a coincidence signal was present or not.

As before, a boron long-counter was used to monitor the neutron flux leaving the target.

2.4A CALIBRATION PROCEDURE

Calibration of the scattered-neutron coincidence system was carried out in four stages as follows.

i) Fast bias setting - crystal

A Caesium-137 source was placed close to the anthracene crystal, and the amplified linear signal was fed through a delay unit to the Northern Scientific analyser, operated in single parameter mode, to produce a pulse-height spectrum. A coincidence signal was derived from the leading-edge fast discriminator output

and fed to the analyser, and coincidence spectra were recorded for various settings of the fast discriminator bias control until an appropriate threshold was reached (see figure 2.5). A comparison of the positions of the low energy cut-off and the high energy falling edge of the Cs-137 electron-recoil spectrum (478 keV electron energy) determine the bias level as 160 keV electron energy, the channel of zero pulse height having been determined as -4 (due to digital gates in the dual ADC). The proton detection threshold is therefore (figure 1.2) 640 keV, which is equivalent to an effective alpha-particle energy of 1.9 MeV.

ii) Fast bias setting - plastic

A linear pulse was derived from the 5th dynode of the photo-multiplier coupled to the plastic scintillator, and the procedure outlined in i) above was carried out for the second detector. The detection threshold obtained corresponded to 120 keV electron energy. The results of Batchelor et al. (1961) for scintillation response in NE 102 have been used to give the corresponding proton energy as 520 keV. The neutron detection threshold is therefore also 520 keV, considering n-p scattering as the sole detection mode (at keV neutron energies this is a good approximation).

iii) Selection of coincidence resolving time

The two detectors, with fast signal bias levels now fixed, were placed so that the phosphors were immediately on either side of a Sodium-22 source. Annihilation gamma rays produced in pairs

and leaving the source at 180° to one another gave rise to simultaneous scintillations in the phosphors. The output of the time-to-amplitude converter shown in figure 2.4 was fed to the multichannel analyser to generate a time spectrum which was recorded in coincidence with a signal derived from the window discriminator driven by the time-to-amplitude converter output. The position and width of the window were adjusted so as to accept scattered neutron flight times up to approximately 10ns . The window width was chosen as narrow as possible to enhance the signal to background ratio of recorded spectra.

Peak A of figure 2.6 was accumulated with the "stop" signal delay as used for recording true coincidence data, while peak B was recorded with the calibrated "stop" signal delay decreased by 9.85ns. It is seen from the rapid fall to zero on the left of peak B that this peak is close to the lower level of the window.

As the flight path was 3.7 ± 2.7 cm, all scattered neutron velocities above about 0.64 cm/ns would be accepted by the window. This velocity corresponds to an energy of 220 keV, which is well below threshold.

The timing resolution of the two biased detectors is seen from peaks A and B to be 5ns for 0.51 MeV gamma rays. This high value is attributed to the fact that a considerable fraction of recoil electrons have energies close to the respective detection thresholds, a situation which, with leading-edge discrimination, inevitably leads to significant jitter. It is expected that the

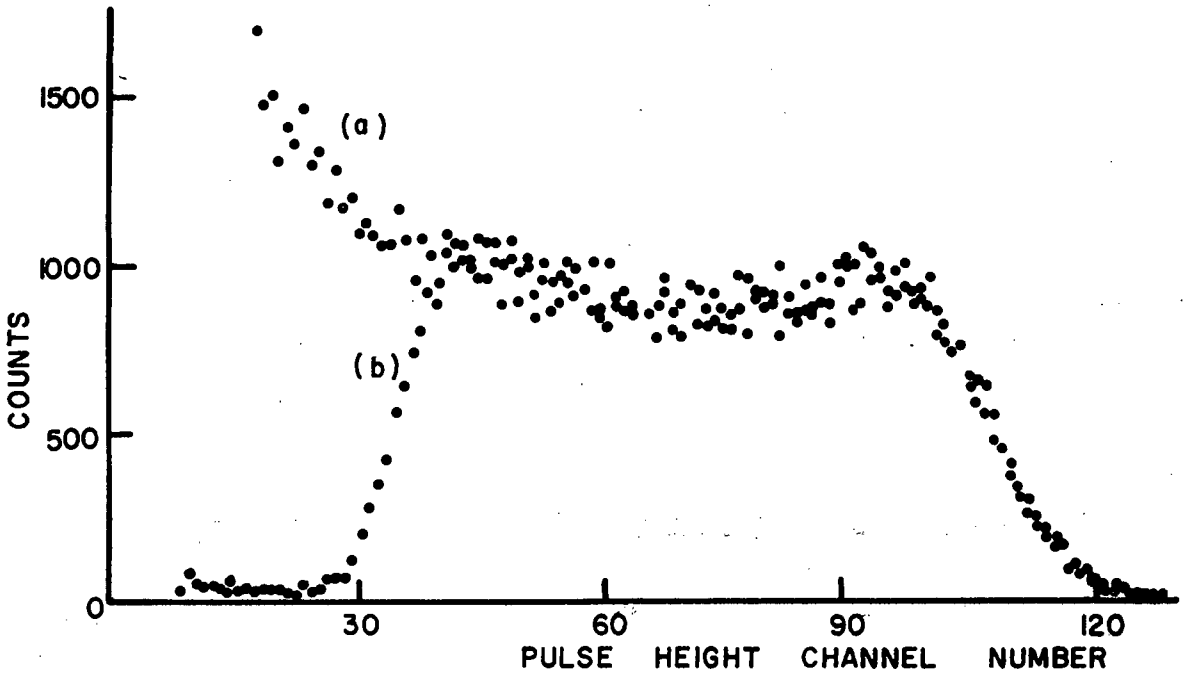

Fig. 2.5 Overlap of Cs - 137 pulse height spectra in anthracene (a) not gated, (b) gated by fast discriminator output.

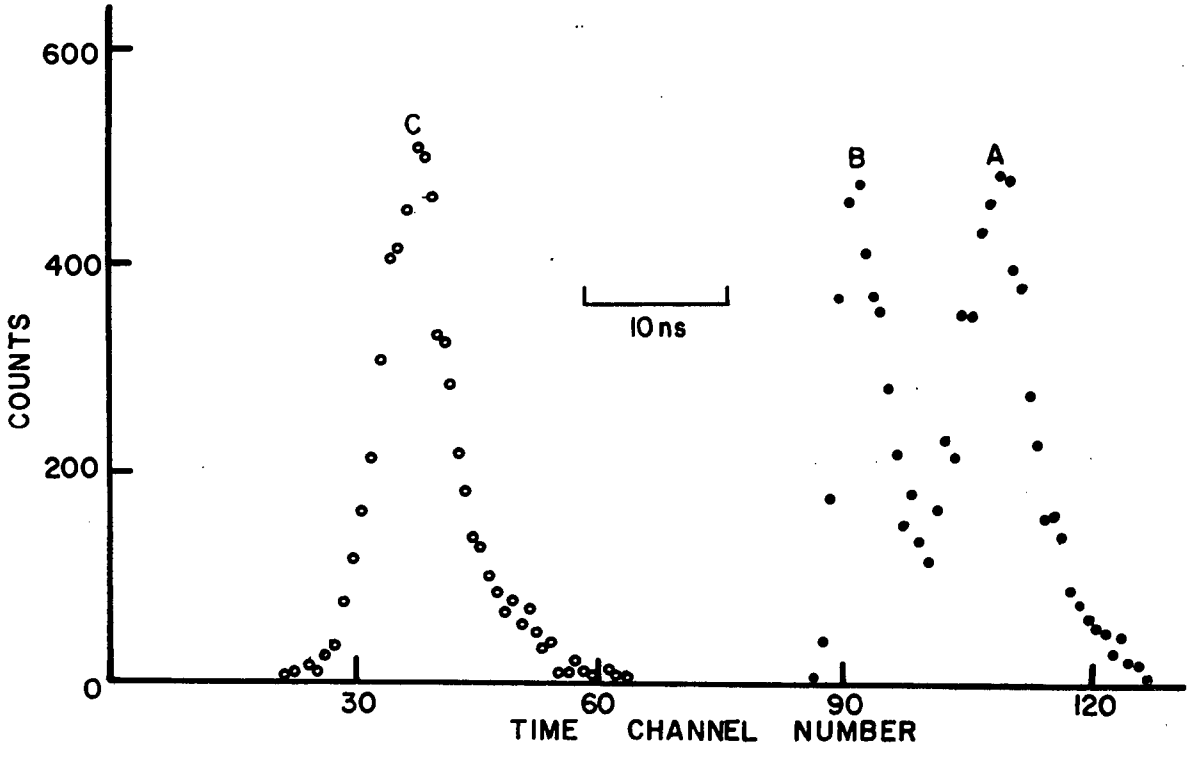

Fig. 2.6 Time spectra for anihilation gamma rays from a Na - 22 sour

resolution for neutrons of energy greater than about 2 MeV will be better than this; nevertheless some loss of counts must occur due to the choice of window width in relation to the resolution.

The "stop" signal delay was decreased by 39.18ns and a gated spectrum recorded. No counts were accumulated. The coincidence requirement was then removed to record peak C of figure 2.6. This value of the "stop" signal delay was adopted as appropriate for measurement of spectra due to random coincidences.

By selecting a different delay rather than adjusting the position of the window, possible alteration of the window width was avoided.

iv) Determination of energy scale

The dual parameter system of Section 2.3 was assembled and an energy scale calibration carried out using a Co-60 source in the same manner as described in Section 2.3.

With the Na-22 source back in position between the phosphors, the linear and gated PSD pulses deriving from the anthracene crystal, and the coincidence signal, were aligned in time using a twin-beam oscilloscope, and the three pulses were fed to the appropriate inputs of the Northern Scientific dual parameter analyser. The detectors were then arranged as in figure 2.4.

The experiments performed with this system and the results obtained are described in Section 3.3.

2.5 NEUTRON TIME OF FLIGHT SYSTEM

In an attempt to determine the cross sections for population of individual excited states of the carbon-12 nucleus in the above experiments, a neutron time of flight spectrometer was assembled. A pulsed deuteron beam was allowed to impinge on the tritium target described above, giving rise to short bursts of neutrons at 500ns intervals. The pulsing was accomplished within the high voltage terminal of the Van der Graaff accelerator. The low energy (few hundred eV) deuteron beam leaving the ion source passed between deflection plates connected to a 2 MHz oscillator, arranged so that the beam was swept in an ellipse. In executing one full ellipse, the beam passed over a small aperture in a plate which otherwise blocked the beam. The transmitted deuteron pulse entered a bunching unit designed by Ortec, whose operation was synchronised to the arrival of the pulse. The bunched pulse was then accelerated by the high voltage of the machine.

A graphite cylinder of length 5.83cm and diameter 2.20cm was suspended by long, fine steel wires from a rigid aluminium support, so that it was a few cm infront of the tritium target, in the horizontal plane defined by the target. A pivot assembly bolted to the floor was positioned directly beneath the graphite cylinder, and a heavily shielded neutron detector was mounted on a trolley and constrained by a rigid steel arm to move in a circle with the pivot as centre. The neutron detector was adjusted to be in the horizontal plane of the target. The detector consisted of a 9.3cm diameter NE213 liquid scintillator mounted on a Philips 58AVP

photomultiplier tube. (See figure 2.7.) A PSD circuit identical to that shown in figure 2.2 was mounted within the aluminium housing enclosing the detector.

A circuit was assembled to measure the energies of neutrons scattered elastically and inelastically by the graphite, by recording their time of flight from the tritium target via the graphite to the liquid scintillator. This time interval was determined by the instant of arrival of a deuteron pulse at the target (detected by an inductive pick-off situated a few cm before the target), and the instant at which a scintillation occurred. A time-to-amplitude converter was used in order that a time of flight spectrum could be recorded in a conventional multichannel analyser. Flight times were recorded only in coincidence with a neutron identification output generated by the pulse shape discrimination circuitry employed. (See figure 2.8.)

2.5A CALIBRATION PROCEDURE

The preliminary steps carried out to convert this system into a quantitative measuring device were as follows.

i) Fast bias setting

The beam pulse repetition time was only 500ns. It was therefore essential to set the overall neutron detection threshold high enough to reject pulses arising from neutrons whose total time of flight was in excess of about 400ns. Consideration of the flight paths from the target to the graphite cylinder, and from there to the detector suggested a desirable threshold of 300 keV.

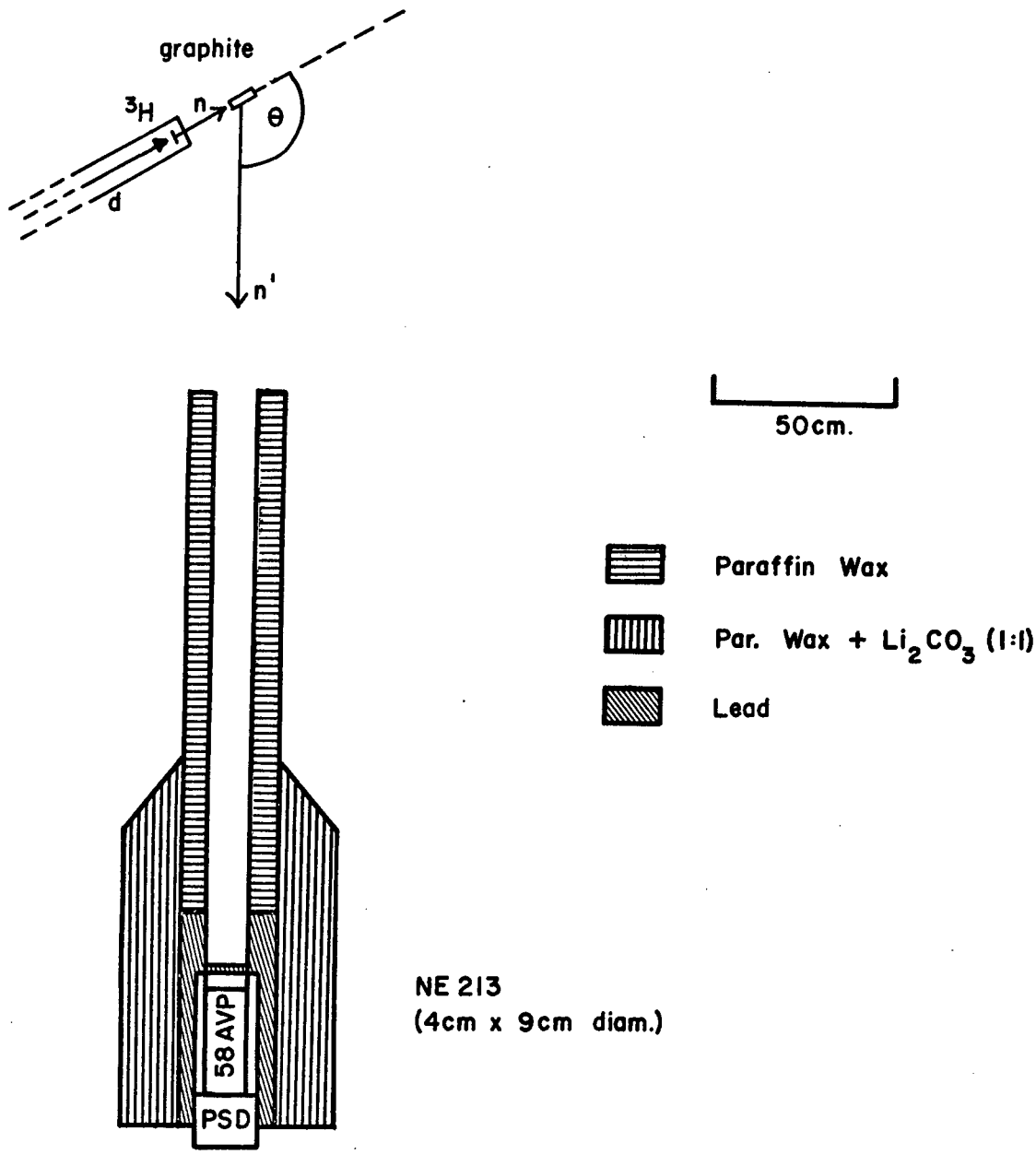

Fig. 2.7 Detector shield construction. Adapted from Jones (1967).

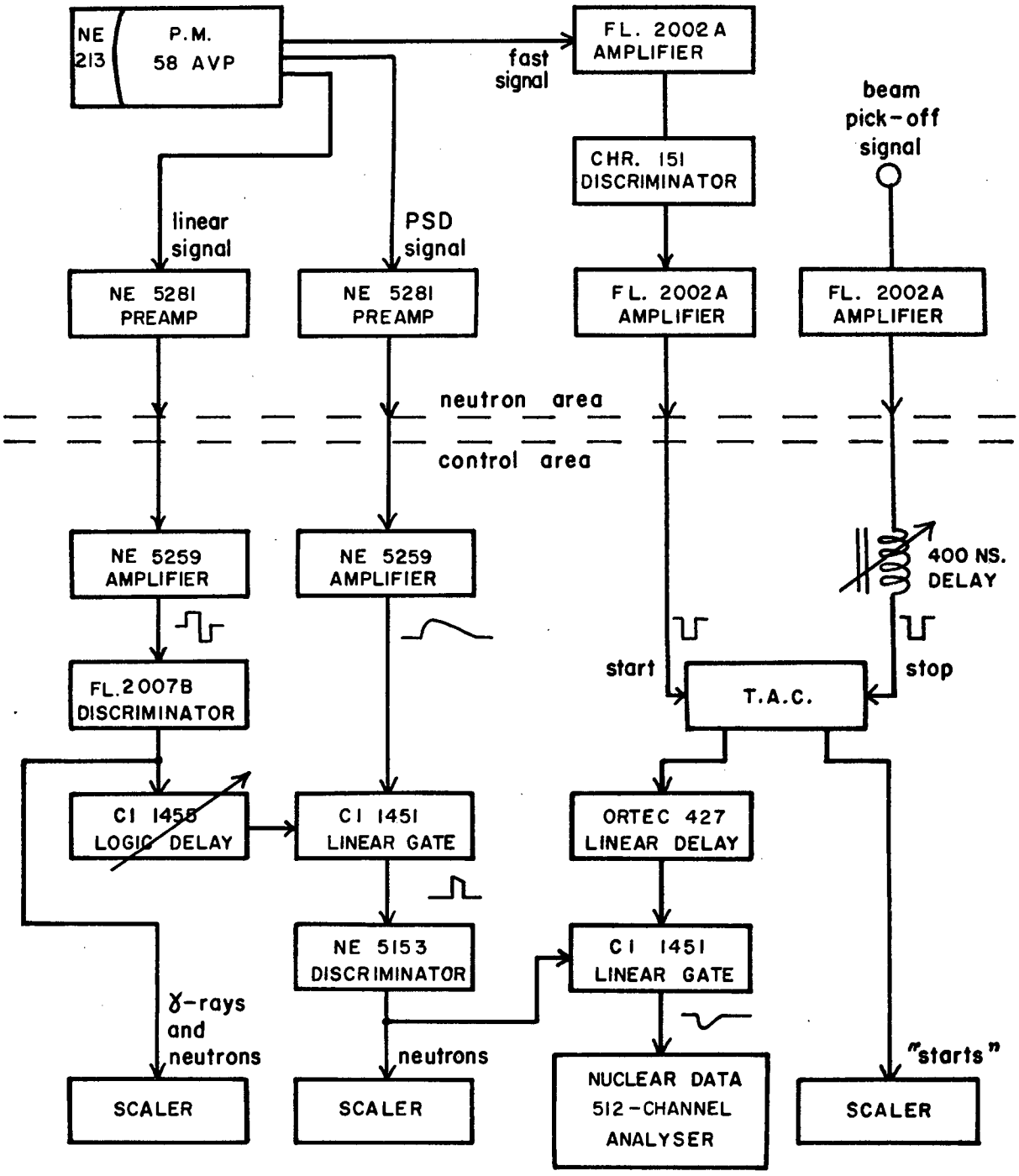

Fig. 2.8 Block diagram of electronic circuit used for $^{12}C(n,n')^{12}C$ neutron time of flight measurements.

The bias level of the fast discriminator was set and recorded using a Cs-137 source. Gated and ungated pulse-height spectra were recorded by a procedure equivalent to that described in Section 2.4A (i). The result is presented in figure 2.9. As the neutron detection efficiency is a sensitive function of the detection threshold in the vicinity of threshold, a correction must be made in the low energy region. This matter is treated in Appendix 2.

ii) Gamma ray discrimination

The pulse shape discrimination part of the system was set up to show electron and proton loci due to an Am-Be neutron source, using a dual pulse-stretcher and X-Y oscilloscope (the Northern Scientific analyser described previously being unavailable). The output of the gated PSD lower-level discriminator (figure 2.8) was used to provide an external "bright-up" signal, and the discrimination level was adjusted so that the entire electron locus was not brightened. After this visual setting-up, pulse-height spectra of a Co-60 gamma ray source were accumulated in a Nuclear Data multichannel analyser, ungated and also gated by the output of the PSD discriminator, and final adjustments were made to the discrimination level so that a gated Co-60 spectrum was just indistinguishable from (gated) background.

The effective neutron detection threshold introduced was calculated from gated and ungated Am-Be pulse height spectra, by comparison with the Am-Be energy spectrum measured by Notarrigo

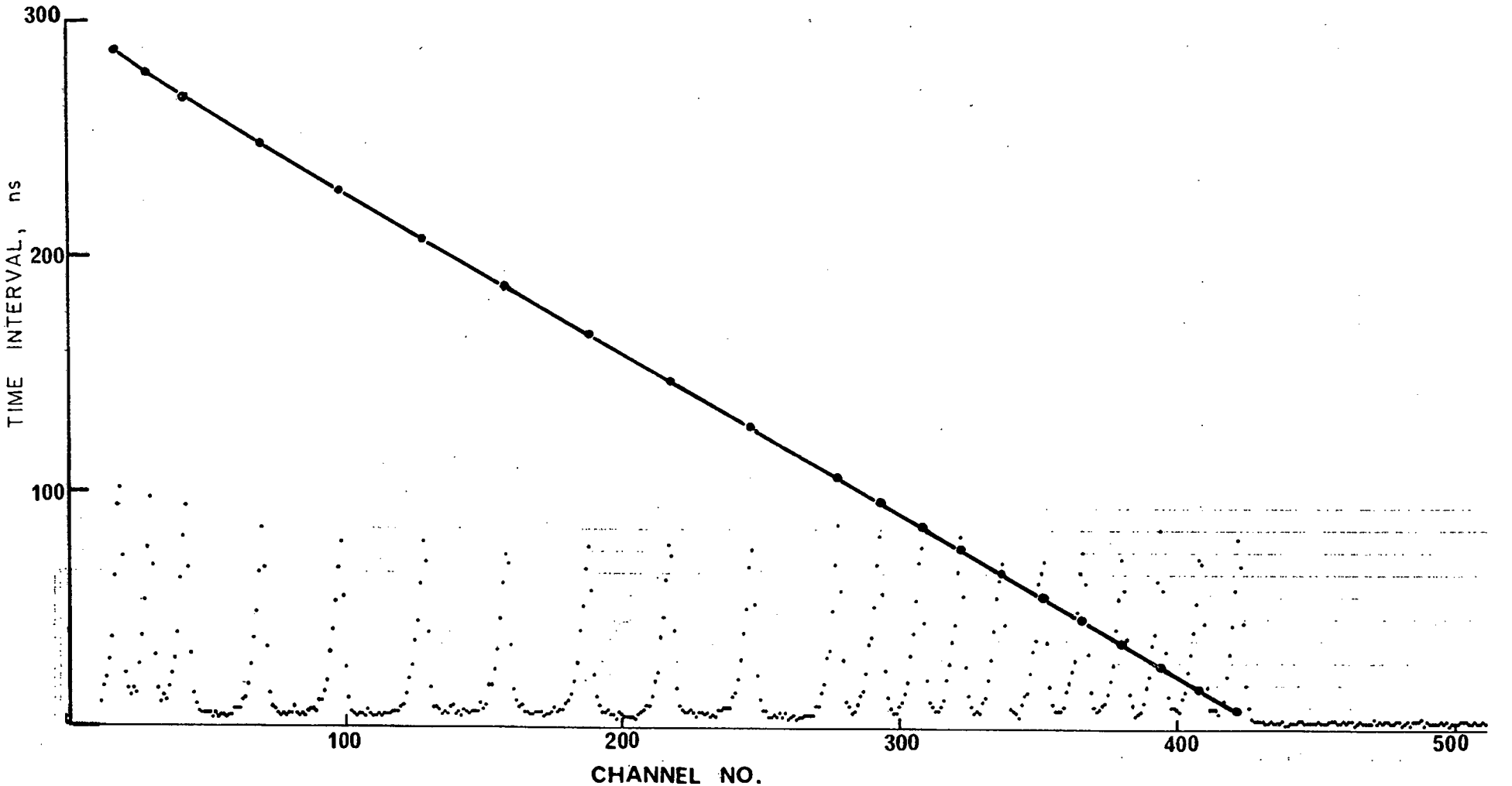

Fig. 2.10 Time scale calibration

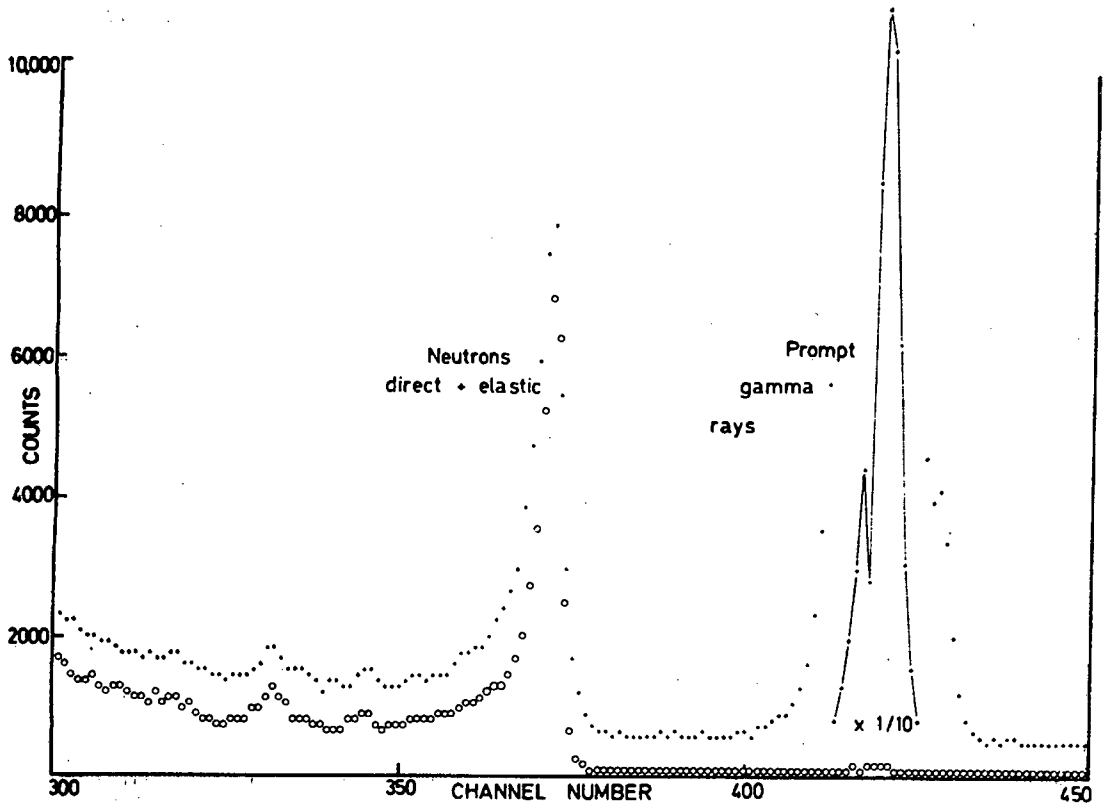

Fig. 2.11 Time of flight spectra. Upper curve, PSD off. Lower curve, PSD on.

the case of 14 MeV neutrons incident on a graphite block of volume more than four times that of the present scatterer. This group found that multiple scattering accounted for less than 20% of the total counts. Comparing the scatterer sizes, it is reasonable to assume that the contribution from multiple scattering in the present case was well below 5% of the number of singly scattered neutrons.

Details of the experiments carried out with this neutron time of flight system are presented in Chapter 4.

CHAPTER 3

MEASUREMENT OF ALPHA SPECTRA

Descriptions are given in this Chapter of the various techniques that were used to obtain pulse height spectra for alpha-particles alone, from data accumulated in fast neutron bombardments of a $1.5cm^3$ anthracene crystal. Within the limits imposed by the particle resolution that was obtained using pulse shape discrimination, an analysis of the results is carried out.

3.1 THE DUAL PARAMETER EXPERIMENT

The experimental system described above in Section 2.3 was assembled to record two parameter spectra arising from fast neutron bombardment of anthracene. The photomultiplier tube was of the type EMI 6097.

Extensive preliminary experimentation was carried out at 22 MeV in order to examine the dependence of the linear and PSD pulse-heights on the crystal orientation with respect to the cone of neutrons incident on it. Two parameter spectra were displayed on the oscilloscope of the 128 x 32 channel analyser. The results agree qualitatively with the findings of Tsukada and Kikuchi (1962) for 3.7 MeV neutrons. The assymetry properties of anthracene were found to affect the alpha-particle locus but little, while the proton recoil locus was seen to undergo significant shifts. The orientation $\theta = 0$ was adopted as that giving the best separation of these two loci.

Energy resolution was limited by the few (128) channels

allocated to its analysis, while only 32 channels were available to accommodate the variation of PSD amplitude. Accordingly, amplifier gain settings and digital gates on the dual parameter multichannel analyser were adjusted to give great prominence to the alpha-particle locus. At this stage the energy scale calibration procedure described in Section 2.2 was carried out.

The energy of the deuteron beam was set at 5.000 MeV, corresponding to a nuclear magnetic resonance frequency of 29.162 MHz in the field monitor of the Van der Graaff's 90° analysing magnet, and was estimated to vary by less than 5 keV throughout the experiment. The beam current was maintained at approximately 1.5 microamperes.

Data were recorded for bombardments at angles $\psi = 0°$, $45°$ and $60°$. In each case the crystal was 18cm distant from the tritium target. The beam current was integrated electronically to yield the total charge reaching the target; the first of these runs was terminated when 10^4 microcoulombs had been counted (taking approximately two hours), while for the second and third runs twice this charge was recorded. The angles given correspond to neutron energies at the phosphor of 22.00, 20.05 and 18.78 MeV respectively, as calculated with the aid of the University's ICT 1301 computer, taking the Q-value for the $^3H(d,n)^4He$ reaction to be 17.58 MeV and using the non-relativistic formula. The values were checked against curves calculated by Goldberg (1963) and found to be in exact agreement.

The contour plot of figure 3.1, derived from the output of

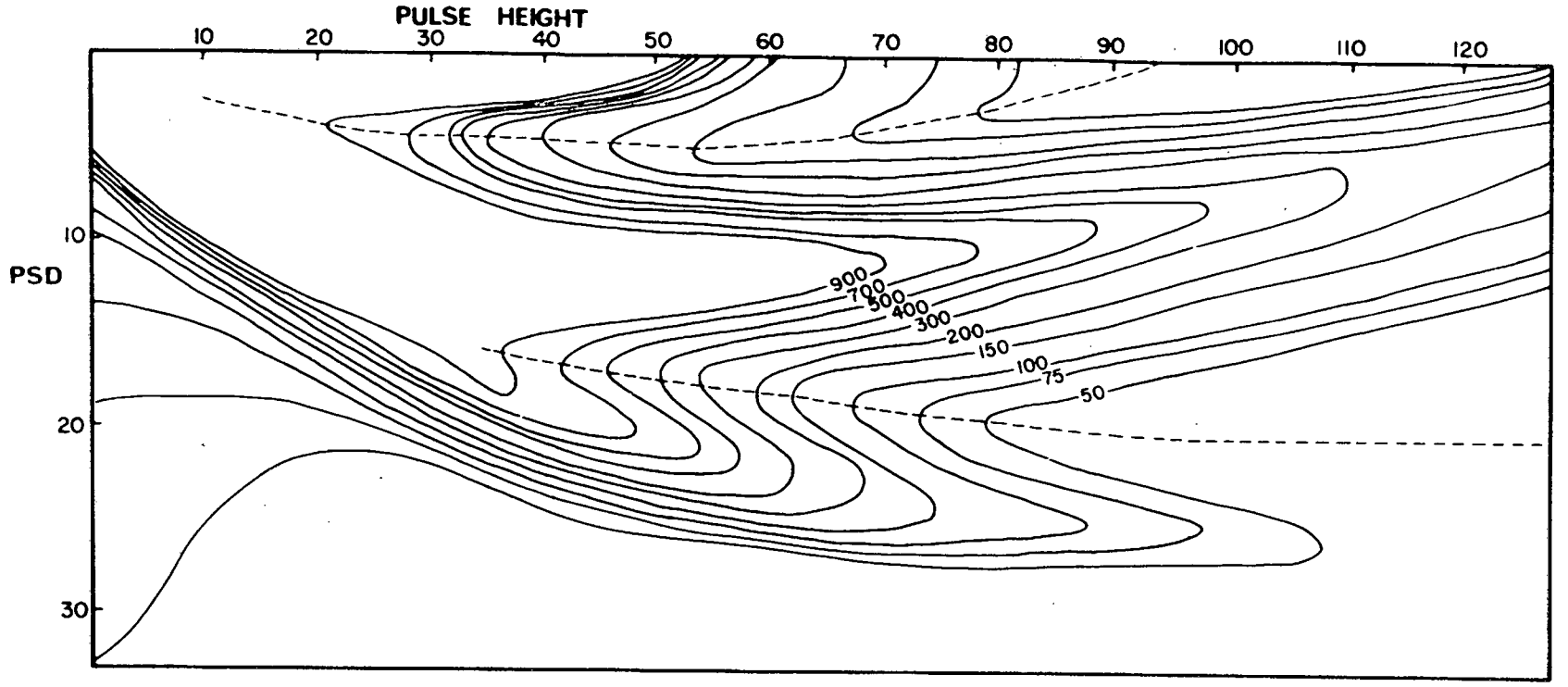

Fig. 3.1 **22.0 MeV NEUTRONS ON ANTHRACENE**
CONTOUR PLOT — COUNTS vs. PULSE HEIGHT vs. PSD

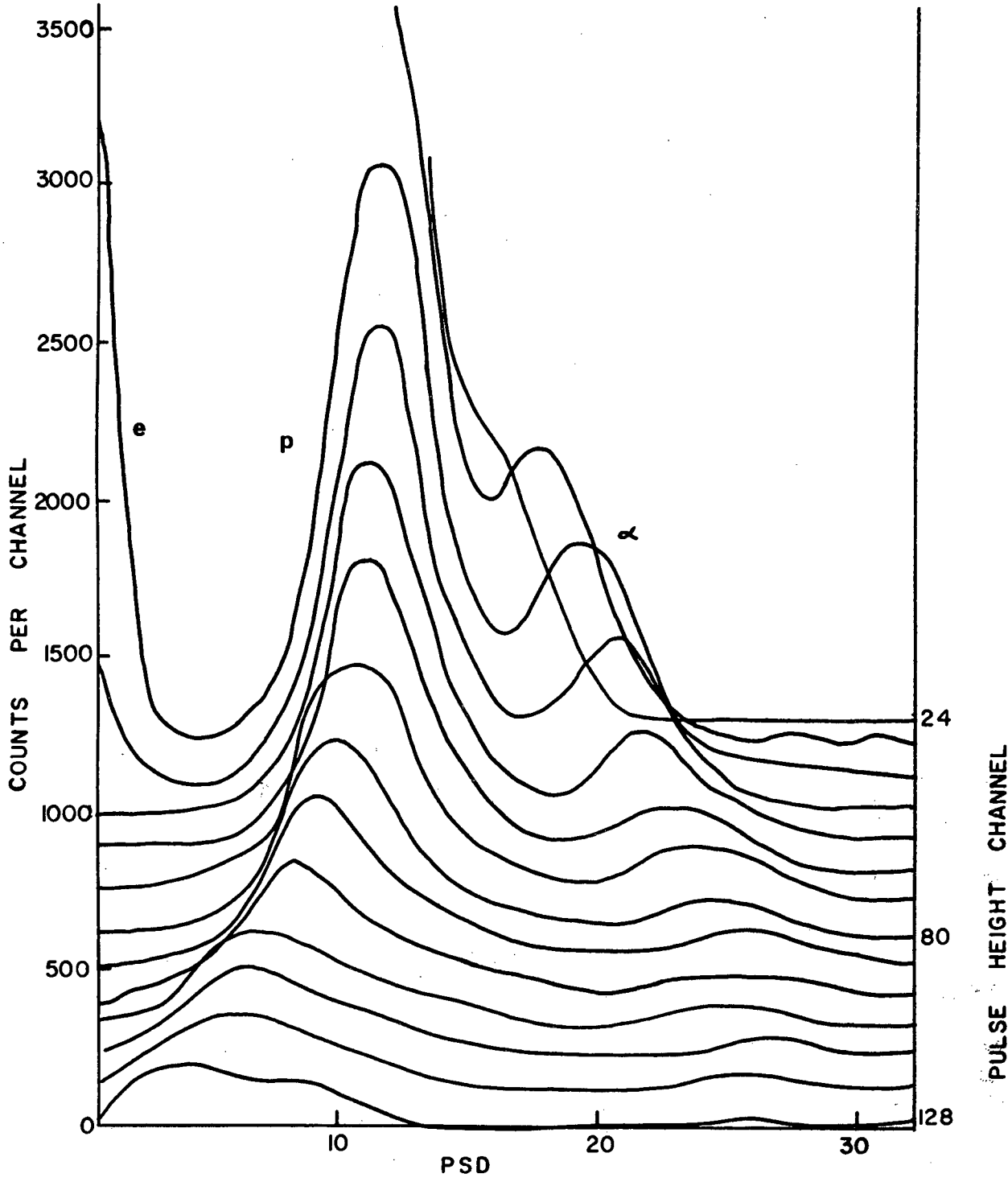

Fig. 3.2 PSD spectra at every eighth pulse height channel. Successive spectra are displaced by 100 counts per channel.

proton spectrum (calculated in Appendix 1) is monotonic. Structure obtained by Johnson was attributed to alpha decays of the C-12 states at 7.65 and 9.63 MeV, and to the $^{12}C(n,\alpha)^{9}Be$ reaction.

In order to remove the proton contribution from the combined proton plus alpha-particle spectrum, two independent approaches were adopted. One was purely numerical, while the other involved subtraction of the calculated theoretical n-p scattering contribution. The numerical approach will be considered here, and the results of both methods discussed in Section 3.3.

It appears (figure 3.2) that towards the low energy region, the proton contribution at each energy channel takes the form of a PSD distribution that is a symmetrical peak. Then the proton contribution may be estimated by calculating the integral of proton counts from the electron-proton minimum up to the proton peak, and multiplying by a factor of 2. The validity of this technique rests heavily on the assumption that the proton contribution at each energy channel is large compared to the respective alpha-particle contribution, an assumption which is seen from figure 3.2 to be well-founded. In the presence of a large number of counts per channel in the region of a peak only a few channels wide, it was essential to determine accurately the position of the peak as a fractional channel value.

A computer program was developed for the University's IBM 1130 computer to implement this technique as follows (program ALPHA, listed in Appendix 4). The stages i) to v) were carried out for the PSD spectrum at each energy channel.

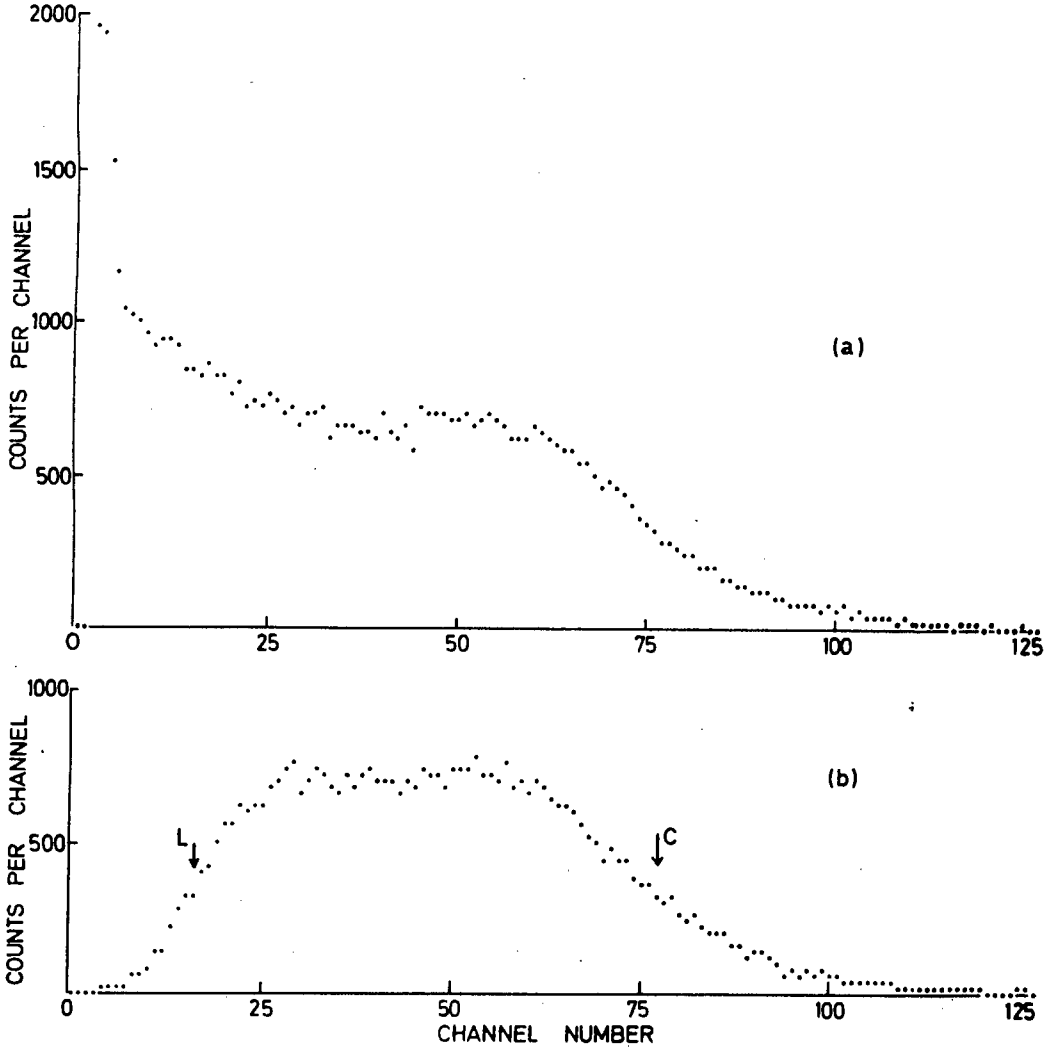

Fig. 2.9 Caesium - 137 pulse height spectra (a) not gated, (b) gated by signal from fast discriminator, showing bias level L in relation to Compton edge C arising from Cs - 137 gamma rays.

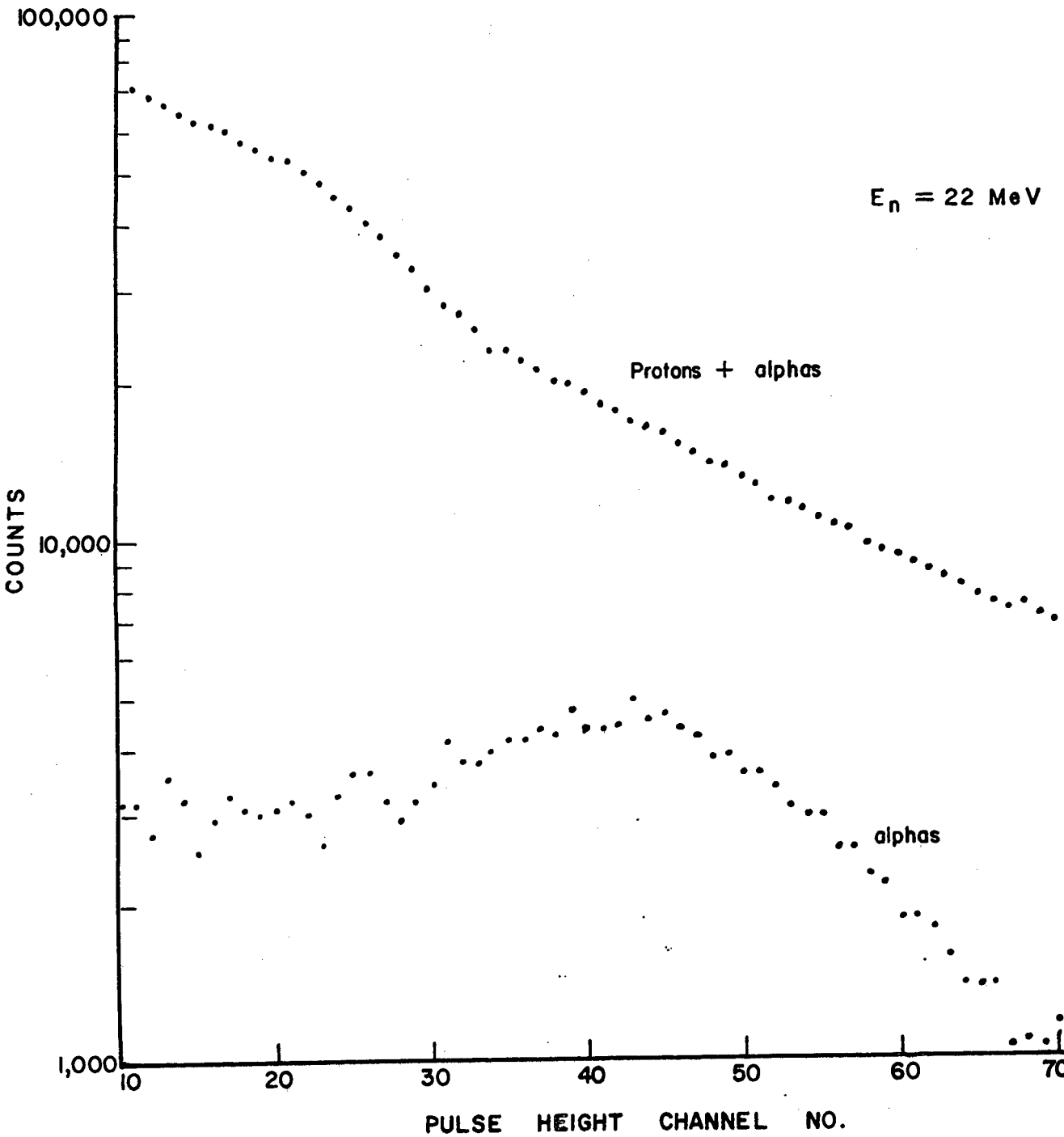

Fig. 3.3 Pulse height spectra generated by the program ALPHA.

Alpha spectra alone are shown in figure 3.4 for the three runs at 22.00, 20.05 and 18.78 MeV respectively. The derivation of the energy calibrations has been described in Section 2.2.

3.3 DISCUSSION OF RESULTS

Figure 3.5 shows a comparison between the proton spectrum as derived numerically from the data and that expected (see Appendix 1) from the n-p differential scattering cross section and the non-linear response of anthracene (figure 1.2), for the 22 MeV case. This discrepency may be due in part to the reaction $^{12}C(n,p)^{12}B$. The transition to the ground state of boron-12 has a Q-value of -12.6 MeV and gives rise to protons of energy between 5.3 and 9.2 MeV in the laboratory frame, while excited final states correspond to protons of lower energy, in the region of the observed high count-rate; the cross section for this reaction, however, decreases from 29mb at 17.5 MeV to 13mb at 19.8 MeV (Jessen et al., 1966), and comparison of these values with the n-p scattering cross-section at 22 MeV suggests that there must be a further source of intermediate energy protons. The (α,p) reaction on carbon-12 (Q = -15.96 MeV) may play a part, the highly energetic gamma rays required arising from electromagnetic C-12 de-excitations as well as from a general gamma ray background. It is likely that an important contribution stems from $^{12}C(n,n')^{12}C^*(p)^{11}B$ reactions. Ten of the known carbon-12 states (Ajzenberg-Selove and Lauritsen, 1968) that can be populated by inelastic scattering at 22 MeV

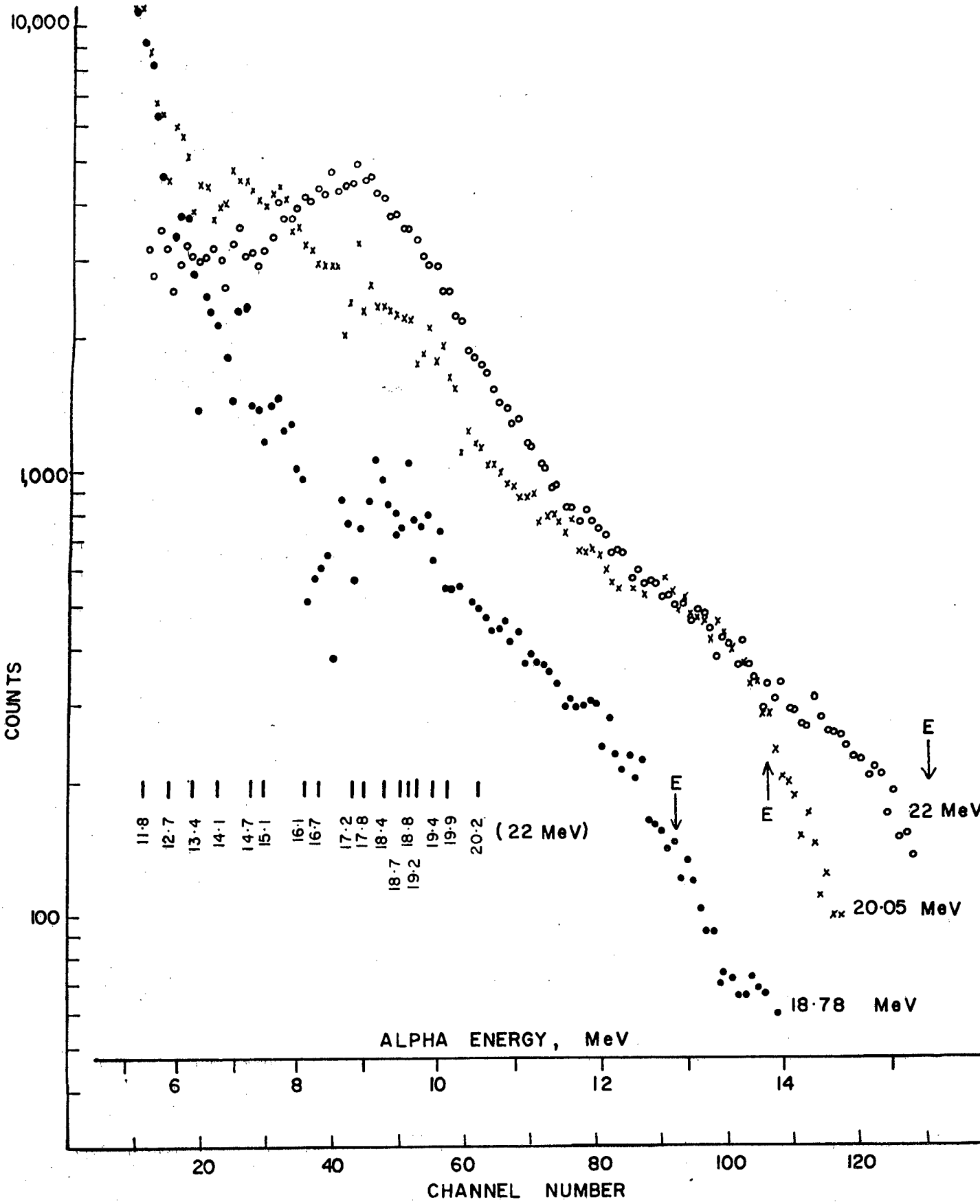

Fig. 3.4 Alpha spectra in anthracene.

have sufficient energy to decay by proton emission, and according to Segel et al. (1965) eight of these have an appreciable proton decay width compared to total width. This reaction mode may produce protons of energy up to 5.57 MeV. It is possible, too, that the beam of neutrons striking the phosphor is contaminated by a low-energy component for which the cross section for scattering from hydrogen nuclei is large (for the energy dependence of this scattering cross section see e.g. Enge, 1966). Such slower neutrons could be due to imperfect focussing of the primary deuteron beam, giving rise to neutron-producing interactions at the tantallum collimators or at one of the magnets on the deuteron line. Because of the uncertainty of the origin and significance of the high proton count-rate at low energy, it was decided to abandon the idea of using alpha-particle spectra obtained from subtraction of the theoretical uncontaminated n-p proton spectrum, and to consider only the numerically generated spectra.

The alpha-particle spectra of figure 3.4 each exhibit complex structure. In order to trace the origin of individual contributions, calculations have been performed for the 3α-disintegration process of each known state in carbon-12, to determine the positions on the spectra at which respective contributions might be expected. For inelastic neutron scattering leading to a particular state of the target nucleus, kinematical considerations indicate the minimum and maximum energies the scattered neutron may have, and hence the maximum and minimum recoil energies, T, of the target. In

the event of the nucleus disintegrating in flight, this recoil energy is added to the characteristic energy of the decay, the whole being distributed as kinetic energy among the three alpha-particles.

The form of the energy distribution may be estimated from the results of phase space arguments. Making the assumption that the disintegration $^{12}C^* \rightarrow 3\alpha$ does not involve the intermediate nucleus ^{8}Be, Frye et al. (1955) have obtained the energy distribution of any one alpha-particle in the carbon-12 centre of mass frame as

$$P(E_\alpha)dE_\alpha = \text{const} \cdot E_\alpha(E_{max} - (3/2)E_\alpha)^{1/2}dE_\alpha$$

where $E_{max} = E_{ex}(^{12}C) - 7.28$ Mev, arising from the -7.28 MeV Q-value for the ground state decay. As this expression is symmetrical about its maximum at $(1/3)E_{max}$, the most probable value of E_α and the mean value coincide at $(1/3)E_{max}$.

Considering only those alpha-particles having this most probable energy, and assuming an isotropic angular distribution in the carbon-12 centre of mass frame, a transformation to the laboratory frame of reference leads to an energy distribution whose maximum is at

$$E_{\alpha lab} = (E_{max} + T)/3,$$

where T is the recoil energy of the excited carbon-12 nucleus. It is therefore reasonable to suppose that the full energy distribution corresponding to each small T interval will be centred at the value given by this expression. (This is to be expected as a direct

result of the principle of conservation of energy and the assumption that the decay mechanism does not differentiate between the three alpha-particles).

With an accurate knowledge of the angular distribution of scattered neutrons leading to a particular energy level in the target nucleus, one could calculate the angular and hence energy distributions for the recoil. The latter would then determine the overall alpha-particle energy distribution. In the absence of such knowledge, the approximation used by Johnson (1963) has been adopted, in that the maximum and minimum values of T have been computed for each state, and the arithmetic mean taken as an estimate of the most probable recoil energy. This approximation gives the maximum of the single alpha-particle energy distribution at

$$E_{\alpha lab} = (E_{ex}(^{12}C) - 7.28 + \frac{1}{2}(T_{min} + T_{max}))/3$$

To arrive at the expected response of the anthracene crystal to three alpha-particles each having this energy, the non-linear response curve (figure 1.2) was used to determine the light output for one particle of this energy, the result obtained being then multiplied by a factor three.

Table 3.1 gives the results of this procedure for the 22 MeV case.

The locations of contributions predicted in this manner have been included in figure 3.4. One additional prediction has been

TABLE 3.1

Energies of particles arising from the $^{12}C(n,n')^{12}C^*$ reaction at 22 MeV.

^{12}C level	Scattered neutron energy		Total energy of 3 alphas			Most probable energy for each alpha	Response to (7)	Effective energy for 3x (8)
	min	max	max	min	mean			
(1)	(2)	(3)	(4)	(5)	(6)	(7)	(8)	(9)
7.65	9.30	14.27	5.42	0.45	2.94	0.98	74	2.5
9.638	7.67	12.23	7.05	2.49	4.77	1.59	128	3.8
10.1	7.38	11.77	7.34	2.95	5.15	1.72	141	4.1
10.844	6.70	10.99	8.02	3.73	5.88	1.96	165	4.6
11.828	5.90	9.97	8.82	4.75	6.79	2.26	200	5.3
12.713	5.20	9.04	9.52	5.67	7.60	2.53	230	5.8
13.352	4.69	8.37	10.03	6.35	8.19	2.73	253	6.3
14.083	4.11	7.59	10.61	7.13	8.86	2.96	280	6.7
14.710	3.63	6.92	11.09	7.80	9.45	3.15	305	7.2
15.109	3.32	6.50	11.40	8.22	9.81	3.27	320	7.4
16.106	2.56	5.42	12.16	9.30	10.73	3.58	360	8.1
16.677	2.21	4.90	12.51	9.82	11.17	3.72	375	8.3
17.23	1.73	4.17	12.99	10.55	11.77	3.92	410	8.8
17.77	1.34	3.56	13.38	11.16	12.27	4.09	420	9.0
18.36	0.94	2.88	13.78	11.84	12.81	4.27	440	9.3
18.39	0.92	2.84	13.80	11.88	12.84	4.28	440	9.3

(continued)

TABLE 3.1 (continued)

(1)	(2)	(3)	(4)	(5)	(6)	(7)	(8)	(9)
18.71	0.71	2.46	14.01	12.26	13.14	4.38	450	9.5
18.84	0.63	2.31	14.09	12.41	13.25	4.42	455	9.6
19.2	0.41	1.86	14.31	12.86	13.59	4.53	470	9.7
19.39	0.30	1.62	14.42	13.10	13.76	4.59	480	9.9
19.88	0.06	0.95	14.66	13.77	14.22	4.74	510	10.2
20.24	0.00	0.03	14.72	14.69	14.71	4.90	530	10.5

included, namely the expected location of the falling edge arising from the reaction $^{12}C(n,\alpha)^{9}Be$. (The contribution of the ^{9}Be scintillation is neglected. This is justified by an extrapolation of the succession of curves in figure 1.2 to heavier ions). For the 22 MeV case, this energy has been calculated as 15.24 MeV; all three predictions are included in the figure, and are labelled E. These positions provide useful calibration points: a slight adjustment of the energy scale has been made.

It is seen from the carbon-12 level density above the level at 9.63 MeV that contributions to the alpha spectra cannot be attributed to the decay of specific individual states. The states may be grouped, however, and regions of each spectrum associated with a group of states. Thus at 22 MeV bombarding energy, for example, two strong contributions are seen to be peaked at approximately 8 and 9 MeV effective alpha-particle energy, and it is reasonable to associate these with the states at 16.106 and 16.577 MeV, and with those from 17.23 to 18.71 MeV, respectively.

Such allocations are, of course, dependent on the validity of the assumption of symmetry for the three alpha-particles emitted in a disintegration, the assumption upon which the energies of Table 3.1 are based. The results of Frye, Rosen and Stewart (1955), obtained from analysis of three-pronged stars produced in a nuclear emulsion irradiated by fast neutrons, have shown that as the bombarding energy increases from 13 to 20 MeV, this assumption approaches the true situation more and more closely. In other words, for high bombarding energies, the role of an intermediate nucleus

(^{8}Be) becomes unimportant to the decay process.

A consideration of the small, positive Q-value for the decay $^{8}Be(g.s.) \rightarrow 2\alpha$ (+0.09 MeV, see figure 1.1) shows that if a state in carbon-12 decays sequentially via the ground state of beryllium-8 to alpha-particles, nearly all the kinetic energy associated with the decay will be taken by the alpha-particle emitted first. The non-linear response of anthracene to alpha-particle energy (figure 1.2) ensures that the total light output of the phosphor will be greater in this case than if the energy were distributid equally among the three alpha-particles produced.

It is suggested that this phenomenon, due to a corresponding non-linear response for stilbene, can be used to explain why alpha-particle groups, detected by Johnson (1963) in pulse-height spectra derived from a stilbene crystal under 14.85 MeV neutron bombardment, were found at pulse-heights about 30% greater than those predicted from calculations equivalent to those of Table 3.1, but neglecting the effects of non-linear response. Had Johnson taken response curves for stilbene into account, the margin of apparent error would have been greater. Comparing the bombarding energy in the stilbene experiment with the 13 to 20 MeV range investigated by Frye et al, it indeed seems likely that the part played by the beryllium-8 nucleus accounts for the observed discrepancy.

In the present experiment it is seen that there is a trend towards population of more highly excited levels as the bombarding

energy is increased. Considered in conjunction with the results of Frye et al. discussed above, this suggests that it is the lower-lying states that decay sequentially via the beryllium-8 nucleus, and that for the disintegration of carbon-12 nuclei in states of high excitation, a single process is preferred.

The cross section for the reaction $^{12}C(n,n')^{12}C^*(3\alpha)$, for a broad range of states considered together, may be calculated from the spectra of figure 3.4, by comparison with the proton spectrum due to n-p scattering, the cross section for the latter process being well-known (Gammel, 1963). This has been done for the 22 MeV case. The theoretical curve of figure 3.5 was integrated over a 1 MeV range, and the fact that the proton energy spectrum is a rectangular distribution was used (see Appendix 1). The formula $C_{14}H_{10}$ for anthracene was taken from Birks (1964). As the crystal was only a few mm. thick (and of non-uniform thickness), no attempt was made to correct for neutron flux attenuation.

It was assumed (Johnson, 1963) that the distribution of alpha-particle energies from the (n,α) reaction was rectangular, and accordingly this contribution, extending from 6.02 to 15.24 MeV, was subtracted as a slowly rising function. The remaining number of events producing apparent alpha-particle energies above 6 MeV gave an estimate for the $^{12}C(n,n')^{12}C^*(3\alpha)$ cross section proceeding via the states from 13.352 to 20.24 MeV excitation energy, of 34 mb. The cross section for the $^{12}C(n,\alpha)^{9}Be$ reaction was obtained as 15 mb.

In calculating the latter value, the alpha-particle contribution

from 6.02 to 15.24 MeV referred to above was used. Thus the assumption was made that beryllium-9 nuclei were always formed in the ground state. This assumption is based on the findings of Frye et al. (1955) for 20 MeV neutrons, although Barjon (1962) reports evidence of excitations of this nucleus to a level at 6.76 MeV when carbon is irradiated with 15 MeV neutrons.

In the following section it is seen how alpha-particle contributions detected in anthracene under 22 MeV neutron bombardment may be associated with specific levels of the carbon-12 nucleus.

3.4 THE COINCIDENCE EXPERIMENT

When the coincidence modification was first devised for the dual parameter system, the motive was to inhibit the storage of n-p scattering data. This modification possesses two major additional features which facilitate the recording of well-defined spectra due to alpha-disintegration of carbon-12 levels only.

The structure of the alpha spectra presented in the previous sections was masked by a broad background due to the (n,α) reaction on carbon-12. Events in the anthracene crystal are now to be recorded only in coincidence with radiations scattered or emitted by the crystal; the recording of (n,α) events leading to the ground state of beryllium-9 will thus be suppressed.

A close analysis of the spectra recorded without the coincidence circuitry was made difficult for a second reason. This was the considerable breadth of individual alpha-particle groups. This breadth

was contributed to by several factors.

Firstly, the non-linear response of anthracene led to the generation of different pulse-heights for different decay channels leading to the same final state. It has been shown in the previous section that this property could in a special case be applied to draw conclusions relating to the channel used. In the present case, however, the non-linearity is responsible for a loss of energy resolution, as a range of distributions of a given energy between three alpha-particles gives rise to a range of pulse-heights.

Secondly, the total kinetic energy of the three alpha-particles emitted in a disintegration of a carbon nucleus at a particular excitation energy, depended on the quantity of kinetic energy imparted to the nucleus by the primary inelastically-scattered neutron. This recoil energy depended on the recoil direction or, equivalently, on the neutron scattering angle.

A third factor introducing a spread of observed pulse-heights is the presence of the inelastically scattered neutron in the crystal. If this neutron undergoes a second collision in the crystal, a significant modification to the pulse height produced could occur. In view of the low detection efficiency of the crystal, however, (the crystal volume was only 1.5 cm^3), this third factor may be expected to have the least serious effect of the three.

The coincidence system described fully in Chapter 2 virtually eliminated the effect of the second of these factors. Only those neutrons whose scattering angle lay in a range of approximately 45°

about a mean value of approximately 135° reached the shielded detector of figure 2.4.

It is probable that the third reason for broadening of alpha peaks described above is affected by the coincidence requirement. For a thicker scatterer this aspect might become significant; it could perhaps be taken into account by using a Monte Carlo calculation approach.

The effects of the phosphor's non-linear response remain unaffected.

The system of Section 2.4 was assembled for the recording of dual parameter data arising from neutron-carbon interactions in the anthracene crystal, and calibrated according to the procedure outlined in Section 2.4A. Two sets of runs were carried out, one with 11 cm of the dense lead alloy described in Section 2.4 interposed between the target and the plastic phosphor, and one with twice this length of shield. The anthracene was positioned directly in front of the target and as close to it as possible within the limits allowed by the geometry in each case. The deuteron beam energy was set at 5 MeV, thus selecting a neutron energy of 22 MeV at the crystal.

Each set consisted of one run with the time-of-flight window (see Section 2.4A) selected to record true coincidences, one run for recording random coincidences only, and a short third run to record data with no coincidence requirement. The duration of the first two runs in each case was approximately three hours.

As the counts accumulated in the background runs were considerable

in each case, it was desirable to introduce some form of numerical smoothing to the data before subtraction of the two-parameter background spectra. The approach adopted for each 32 x 128 channel array was to smooth each 32-element PSD spectrum by the method of fourth differences (see Appendix 3). The method required the fitting of several thousand least-squares parabolas per run, and it was decided to write a computer program to carry out the numerical procedures involved (see program MDIFF, Appendix 4). Both the true coincidence and random coincidence runs were smoothed before subtraction. The number of counts recorded by the boron long counter for each run was used to normalise the random coincidence spectrum to the real coincidence spectrum in each case.

For the case where the greater length of shield was used to screen the plastic from the neutron source, it was found that the signal to background ratio in the region of interest was low. The result was that in the region of interest of the net matrix, obtained by subtraction after smoothing, the statistical errors were similar in magnitude to the respective counts. This was not so for the case in which the thinner shield was used. The interpretation is that there was a high flux of background radiation in the general vicinity of the neutron source, whose dependence on distance from the source was much less sensitive than inverse square dependence. This would arise from neutron scattering at the bulky liquid nitrogen tank and cold trap assembly, and at the ceiling, floor and walls of the neutron area (the nearest

wall was of concrete, 2 metres from the target) and from gamma ray production at the deuteron beam collimators and elsewhere.

It was found that due to a relatively low ratio of proton counts to alpha-particle counts in the matrix generated by the program MDIFF, the loci for these two groups were readily separable, without resorting to the techniques used in the computer program ALPHA, to an alpha-particle energy as low as 4 MeV. In figure 3.6, the pulse height distribution of counts recorded in the alpha-particle locus of this matrix is presented, for the data set recorded at the closer distance from the target. The errors given represent the sum of counting errors for the two runs.

The data accumulated with the coincidence switched off were used to provide the 15.24 MeV alpha-particle energy calibration point referred to in Section 3.3. The energy scale calibration calculated from a Co-60 spectrum measurement, was confirmed.

The positions marked above the experimental points in figure 3.6 refer to the expected positions of alpha groups. They have been calculated using the technique of Section 3.3, but for the range of n-C scattering angles appropriate to the geometry of the coincidence experiment. This angular range was taken to be $135^{\circ} \pm 23^{\circ}$. A shift in expected peak location of up to 1.4 MeV results from this restriction of the scattering angle. Table 3.2 shows how the results were obtained.

It appears from figure 3.6 that the carbon-12 states of excitation energy from 7.65 to 13.352 MeV all play a significant part in

TABLE 3.2

Energies of particles

arising from the $^{12}C(n,n')^{12}C^*$ reaction at 22 MeV.

Neutron scattering angle 135°

^{12}C level	Scattered neutron energy	Total energy of 3 alphas	Most probable energy for each alpha	Response to (4)	Effective energy for 3x (5)
(1)	(2)	(3)	(4)	(5)	(6)
7.65	9.73	4.99	1.66	135	3.9
9.638	8.06	6.66	2.22	195	5.2
10.1	7.67	7.05	2.35	210	5.5
10.844	7.06	7.66	2.55	232	5.8
11.828	6.24	8.48	2.83	264	6.5
12.713	5.51	9.21	3.07	295	7.0
13.352	4.99	9.73	3.24	315	7.3
14.083	4.39	10.33	3.44	344	7.8
14.710	3.88	10.84	3.61	360	8.1
15.109	3.56	11.16	3.72	375	8.3
16.106	2.77	11.95	3.98	414	8.9
16.577	2.40	12.32	4.11	422	9.0
17.23	1.90	12.82	4.27	440	9.3
17.77	1.49	13.23	4.41	455	9.6
18.36	1.06	13.66	4.55	472	9.7
18.39	1.04	13.68	4.56	473	9.7
18.71	.81	13.91	4.64	490	10.0
18.84	.72	14.00	4.67	494	10.0
19.2	.48	14.24	4.75	511	10.2
19.39	.36	14.36	4.79	520	10.4
19.88	.08	14.64	4.88	540	10.7
20.24	-	-	-	-	-

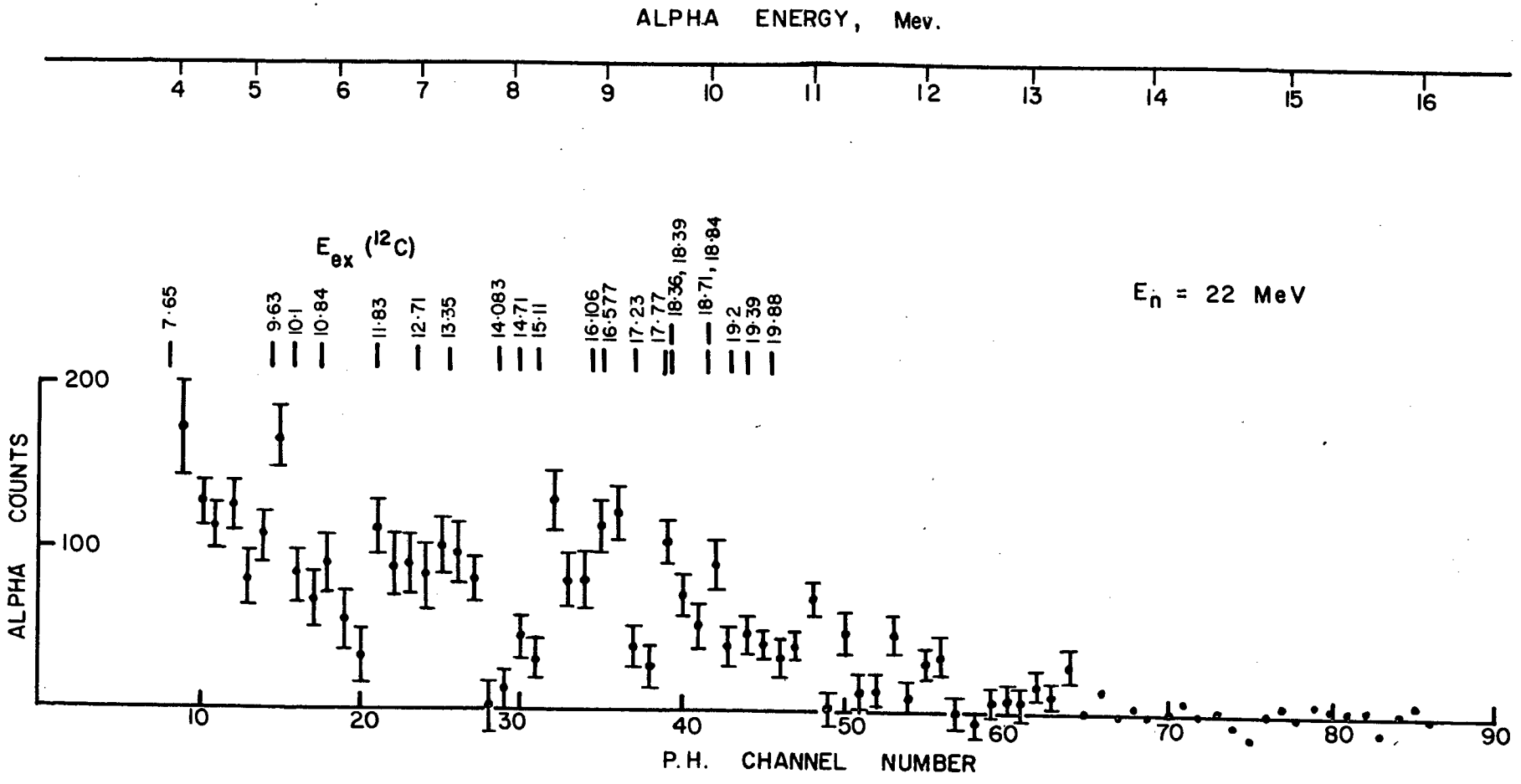

Fig. 3.6 Coincidence alpha spectrum in anthracene.

the reaction $^{12}C(n,n')3\alpha$ at 22 MeV. The presence of a broad band of alpha-particle energies corrseponding to a level in the vicinity of 10.1 MeV excitation can not be isolated with certainty, although the single high count in channel 15 does appear to reside on a broad group extending from 6 MeV apparent alpha-particle energy down towards lower energies.

Many states of excitation energy greater than 13.352 MeV appear to contribute to the spectrum at higher energies. In particular the pair of levels at 16.106 and 16.577 MeV may be associated with the peak at channels 35 and 36. For still higher-lying levels it is difficult to make specific allocations; for levels of excitation greater than about 18.5 MeV, it is important to note that the scattered neutrons have energy near the detection threshold of the plastic phosphor, resulting in a loss of detection efficiency. The efficiency of this biased detector has not been investigated in detail (cf. Appendix 2), as the geometry calls for a highly sophisticated treatment. A Monte Carlo calculation approach similar to that of Batchelor et al. (1961) or Joseph et al. (1967) would provide an appropriate method.

As a check on the data smoothing and alpha-proton separation processes, the proton pulse-height spectrum of the net matrix has been examined. Marked structure is seen for proton energies below about 7 MeV (figure 3.7).

Much of this structure has been accounted for by consideration of the reaction $^{12}C(n,n')^{12}C^*(p)^{11}B(g.s.)$. The calculation of expected proton group locations, in terms of proton energy, is outlined below.

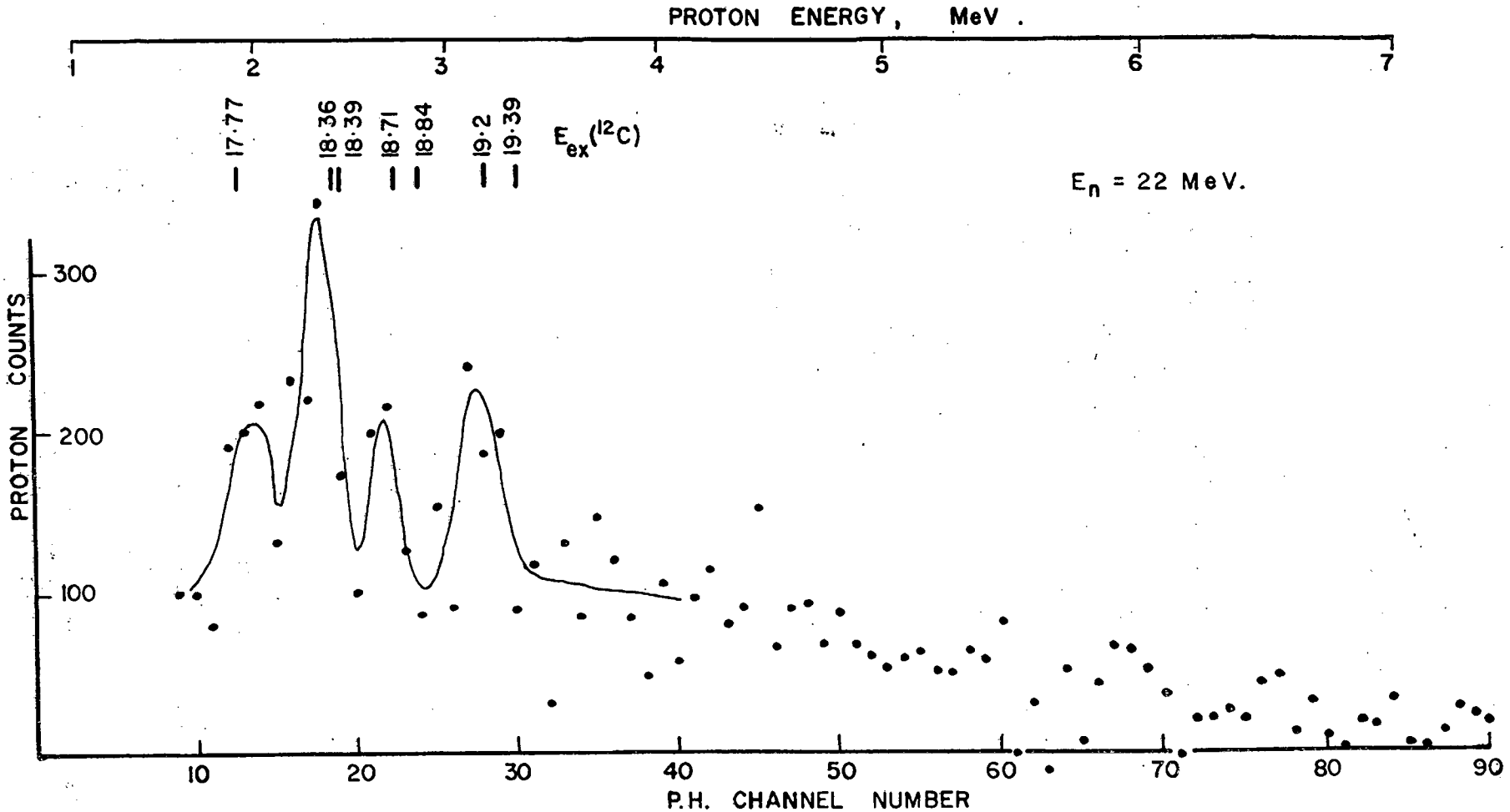

Fig. 3.7 Coincidence proton spectrum in anthracene.

previous section.

It must be pointed out that the results obtained with the system used in the coincidence experiment are subject to one source of ambiguity. Gamma rays produced by fast neutron interactions in the anthracene crystal, if detected in the plastic, can produce a "real" coincidence signal. Thus some alpha-particles from the reaction $^{12}C(n,\alpha)^{9}Be^{*}(\gamma)^{9}Be$, if it occurs (Frye et al. 1955, Barjon et al. 1962), could be included in the spectrum of figure 3.6. Or, if a decay such as $^{12}C^{*}(\gamma,3\alpha)$ occurred, the coincidence signal corresponding to the process would be generated with exaggerated efficiency.

Two extensions of the system used in the present case could be employed to discriminate against such gamma rays. A longer scattered-neutron flight path could be used in conjunction with a time-of-flight discriminator; or pulse shape discrimination could be applied to the scattered-neutron detector. At an early stage of the present investigation, a system incorporating both of these features was designed and assembled; its full operation, however, required a triple parameter data storage system, to accumulate information relating to pulse height, pulse shape, and scattered-neutron time of flight for each scintillation in the scatterer fulfilling an appropriate fast coincidence requirement. A four parameter digital data storage system has since been constructed and is to be used in the three parameter experiment described above. Due to pressure of time, this experiment has had to fall outside the scope of this thesis.

CHAPTER 4.

MEASUREMENT OF NEUTRON SCATTERING CROSS SECTIONS

A unique interpretation of the alpha-particle spectra obtained by the methods of Chapter 3 was hampered by the close spacing of the carbon-12 levels involved. The aim of this neutron time-of-flight experiment was to attempt to determine angular distributions for inelastic scattering on individual highly excited states of the carbon-12 nucleus, leading to cross sections for the respective processes. It would appear (BNL 400, 1970) that no such data exist for neutron energies near 22 MeV. It was expected that this knowledge would define more closely the states whose alpha-decays were observed in previous experiments, and lead to an estimation of branching ratios for alpha-particle, proton, and hence also gamma ray decays of excited states of the nucleus of interest.

In point of fact the results were somewhat inconclusive. Section 4.3 is devoted to a discussion of why this was so, and of possible ways in which the experiment could be improved. A proposed multiparameter time-of-flight experiment is discussed. First of all, however, the experiment is described as it was performed.

4.1 THE NEUTRON TIME OF FLIGHT EXPERIMENT

Using the system described in Sections 2.5 and 2.5A, time of flight spectra were recorded for monoenergetic neutrons scattered by carbon. Spectra were accumulated in pairs for five values of the laboratory scattering angle, ranging from 37° to 142°, one with the graphite cylinder in position, and one with it removed to record the neutron background, at each angle. The flight path was 2.47m in each case. Sets of ten spectra were recorded for two values of the

incident neutron energy, namely 22.00 and 20.05 MeV.

For the first set of spectra, the deuteron ion source used in the Van der Graaff accelerator was of the radio-frequency plasma-generation type, and the timing resolution was 3ns as already shown. At the time of lowering the deuteron energy for the second set of ten spectra, an Ortec duoplasmatron ion source was substituted for the RF source. The time scale was recalibrated from delayed prompt gamma ray peaks, recorded with the PSD switched off, and the timing resolution was now found to be 5ns. The effect of this deterioration was compensated for to some extent by the fact that flight times of slower neutrons were now being recorded. A recalibration of the time scale was necessary as slower deuterons were to traverse the finite distance between the inductive pulse pick-off and the tritium target.

A typical pair of spectra obtained from scattering of 22 MeV neutrons is shown in figure 4.1. The counts from channel number 400 to 500 were summed for each spectrum, and the entire background spectrum multiplied by the normalising factor required to make the 100-channel sums equal.

In spite of the very poor signal-to-background ratio reflected in figure 4.1, an attempt was made to subtract the background spectrum, to obtain the contribution of n-C scattering to the whole. It was essential to apply some form of numerical smoothing to the data before subtraction; on the other hand there is clearly a good deal of structure in the background spectrum which prohibits the use of "global" smoothing techniques. The local smoothing technique known as the

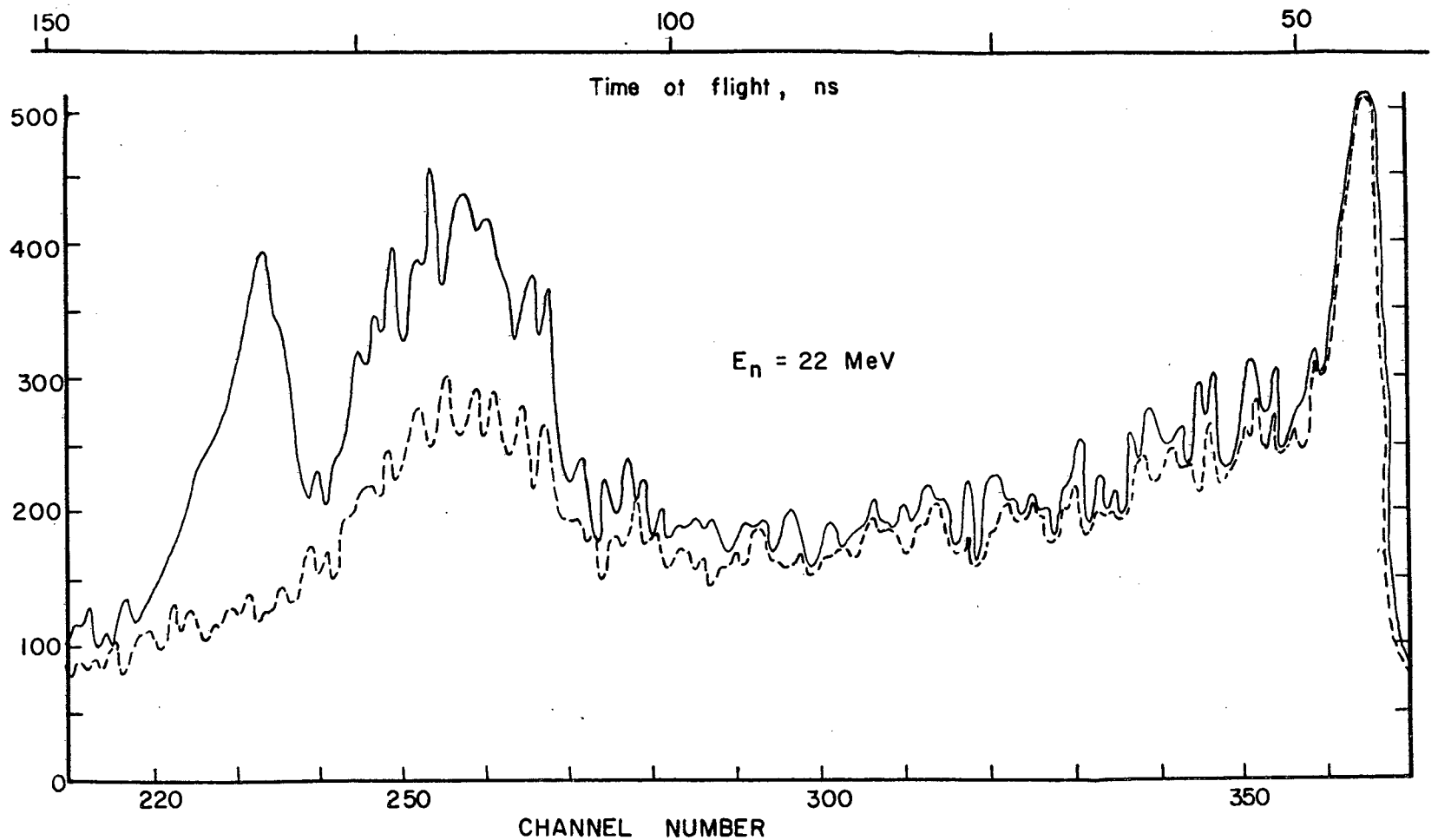

Fig. 4.1 Neutron time of flight spectra (----background) at 142°.

method of fourth differences (see Lanczos, 1957) was adopted, and is described in Appendix 3. Each spectrum of each pair was smoothed before subtraction. The difference between the spectra of figure 4.1 is shown in figure 4.2. Computer subroutines SMOOV and GRAPH (see Appendix 4.3) were written for the University's IBM 1130 computer to implement the smoothing and to give a visual presentation of the various spectra.

As a check on the possibility of the time scale altering due to drifts in the electronic circuits, each run was immediately followed by a short run with the PSD switched off, to record the position of the prompt gamma ray peak. In no case was the error determined in this fashion greater than one channel. The expected position of the peak due to neutrons proceeding directly from the tritium target through the shield to the neutron detector was also calculated for every spectrum. A peak was found within one channel of the expected position in every case. This result indicates that the neutron shield provided inadequate screening of the liquid scintillator.

4.2 DISCUSSION OF RESULTS

A calculation was performed with the aid of the University's ICT 1301 computer to determine the expected positions on each of the time of flight spectra of neutron groups corresponding to the levels of carbon-12 that may be excited in the scattering sample. Calculated positions are shown for the spectrum of figure 4.2.

It is seen from the magnitude of the counting errors in this figure that no meaningful results for the number of counts corres-

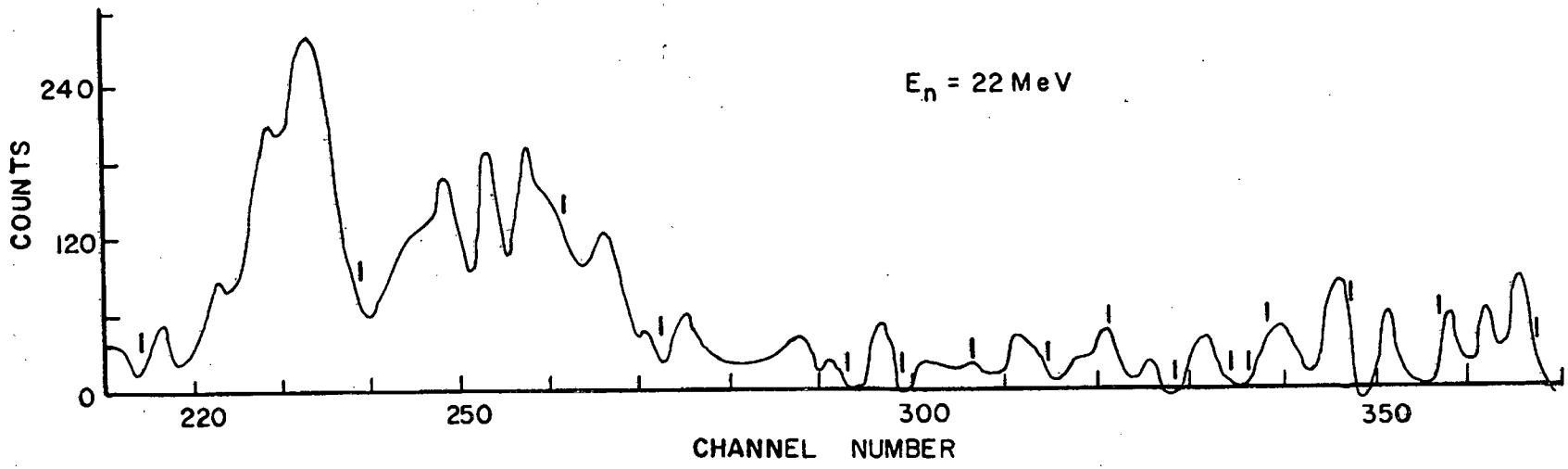

Fig. 4.2 Neutron time of flight spectrum at 142° after subtraction of background.

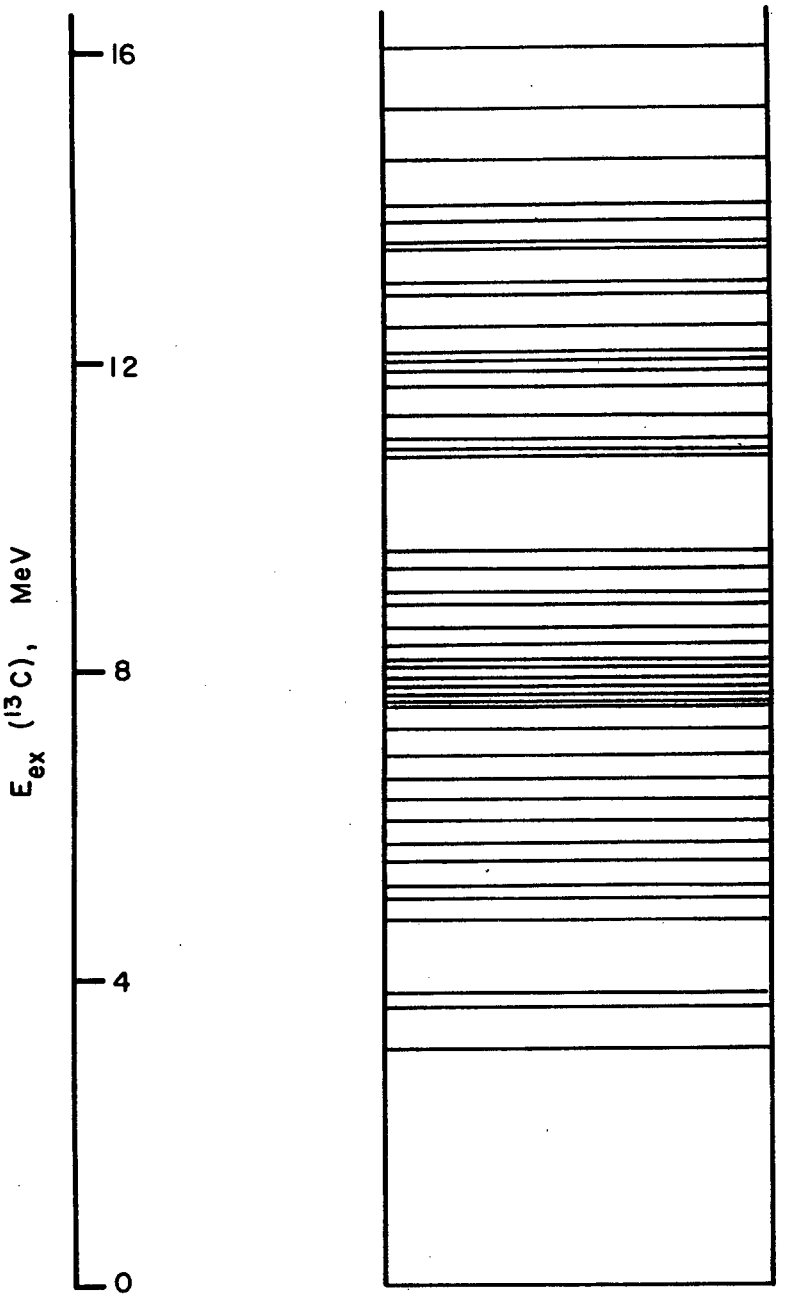

Fig. 4.3 Energy levels of Carbon – 13.

to provide a neutron flux able to compete with the background flux.

3. The shield was inadequate for screening fast neutrons. This is seen from the presence of a peak due to direct neutrons in every spectrum.

4. The neutron spectrum leaving the target vicinity was not entirely monochromatic, as seen from the run intended for permitting normalisation of data to absolute cross sections (Section 2.5A)

5. Too long a flight path was chosen in relation to the scatterer size; equivalently, the timing resolution (3ns) was too poor. This was due to:

   i) The deuteron pulses being too broad.

   ii) As the fast anode pulse from the photomultiplier was required for pulse shape discrimination purposes, a slower dynode pulse was used to trigger the fast discriminator.

   iii) Discriminators operating on the amplitude of the leading edge of a pulse (as used here) cannot provide a high order of resolution in the presence of a broad spectrum of pulse heights.

Methods are in fact available for avoiding most of the above undesirable phenomena. Firstly, of course, the neutron scattering area should be large, and ideally of light construction.

A shield of intermediate screening properties is most undesirable. That used in the present experiement could be exchanged for a more

effective shield, or alternatively, if the neutron area were sufficiently large, an open geometry could be used.

The method of defining the starting time of a neutron's flight from the tritium target via the scatterer to the detector used here (i.e. inductive beam pick-off) has been improved upon by Barjon et al. (1962), Grin et al. (1965) and others, who have employed a counter situated in the accelerator vacuum to detect the production of alpha-particles in the $^{3}H(d,n)^{4}He$ reaction.

The timing resolution may be further improved by using a detector consisting of two photomultipliers viewing the same scintillator, one equipped with a PSD circuit, while the anode of the second tube is available for fast timing purposes. The tubes may be operated in coincidence and biased into the noise region to improve leading-edge discrimination (Batchelor et al. 1961) or better, a cross-over timing discriminator may be used instead.

A significant modification to neutron time of flight studies in the case of a carbon scatterer was introduced by Grin et al. (1965). The technique was to use two organic plastic scintillators, one as the neutron scatterer and the other to detect the scattered neutrons. Grin et al. estimated that as little as 10% of background radiation was recorded when this technique was used. This Lausanne group applied pulse shape discrimination to the neutron detector to eliminate gamma ray background, while amplitude discrimination was applied to the scatterer in order to select either those events producing low pulse-height carbon recoil scintillations, or those giving rise to alpha-

particles producing a somewhat higher range of pulse-heights. The bombarding energy was 14 MeV. Similar spectra were obtained for the two cases, except that the 9.63 MeV level was always seen to decay by alpha-particle emission.

As mentioned briefly at the close of Chapter 3, an experiment similar to that last mentioned is to be performed at S.U.N.I. The emphasis will be somewhat different, however. Pulse shape discrimination will be applied to the scatterer, to distinguish alpha-particle disintegrations from processes that give rise to protons. PSD applied to the second counter will serve to discriminate against gamma ray induced scintillations. Scattered neutron energies will be recorded by measurement of the true time of flight between the scintillators. The recording of three numbers per event, generated from the linear and gated PSD signals of the scatterer, and the neutron flight time, is envisaged. The magnetic tape multiparameter data storage system constructed at U.C.T. is to be used to accumulate the data. Successive replays of the magnetic tape should permit a two parameter pulse-height-PSD display to be generated for each excited state of carbon-12 populated, for level densities where timing resolution permits this.

On the basis of the excellent background suppression results of Grin et al. (1965, 1966, 1969), it is confidently hoped that the multiparameter neutron time-of-flight spectrometer to be used at 22 MeV will provide effective reduction of the background count rate; although background radiation effects may be expected to be more serious at the higher bombarding energy.

CHAPTER 5

SUMMARY

The pulse shape discrimination technique of particle identification in an organic phosphor has been effectively extended to distinguish reactions involving alpha-particles from other events in anthracene.

Resolution of particle type was found to be a sensitive function of the particle energies. Proton-gamma-ray resolution at a fraction of 1 MeV proton energy has been attainable for some time (Brooks, Pringle and Funt, 1960). The proton-alpha-particle resolution has been extended down to a proton energy of approximately 2 MeV, or 5 MeV apparent alpha-particle energy, by a numerical technique.

At the high neutron bombarding energies used, the accuracy of numerical methods for analysis of the low-energy data region was jeopardised by an excessive proton event count-rate. More than a general interpretation of the alpha spectra was further inhibited by recoil energy spread of decaying nuclei, and the presence of the (n,α) background contribution.

These undesirable effects were annulled by the introduction of a second detector, alpha-particle and proton energy spectra being then readily obtained. Particle resolution was now unambiguously extended down to 1.5 MeV proton energy (4 MeV apparent alpha-particle energy).

The results of phase-space symmetry arguments, and kinematical considerations, combined with a knowledge of the anthracene light output as a function of particle type and energy, were

sufficient to attribute structure in the spectra obtained to particle decays of individual carbon-12 states proceeding via alpha-particle and proton emission respectively. Some indication has been found of a broad level near 10 MeV excitation energy.

For the structure of such spectra to be well defined, it is desirable that the second (coincidence) detector subtend a small range of the scattering angle at the scatterer. Effective background suppression, however, requires the solid angle subtended by this detector to be large. It is therefore suggested that the geometry of this experiment could be improved by substituting a symmetrical annular scintillator for the present cylindrical shape. For adequate light collection, the second detector should then comprise two photomultipliers. One of these could be used to provide pulse shape discrimination, to discriminate against possible contaminating reactions, and to reduce the background contribution still further. The anode signal from the remaining tube would then be available for fast coincidence purposes. The experience of the time-of-flight experiment suggests that an open geometry should be maintained, a single conical shield being used for screening from the neutron source. The annular scintillator could be a plastic, appropriately machined to facilitate a straightforward efficiency calculation.

The causes of an excessive background contribution bave been discussed for a neutron time of flight experiment. A revised

approach has been suggested, incorporating a many-parameter analyser, of a type described in detail by Egelstaff and Rae (1964).

APPENDIX 1

PROTON RECOIL SPECTRUM

DUE TO

N-P SCATTERING IN ANTHRACENE

The differential cross section for n-p scattering may be described by the result of[a] partial wave analysis of the elastic scattering process. The scattering amplitude obtained is

$$f(\theta) = (1/k) \sum_{\ell=0}^{\infty} (2\ell + 1)\, e^{i\delta_\ell} \sin\delta_\ell \; P_\ell(\cos\theta)$$

and the differential scattering cross section is given by

$$d\sigma/d\Omega_{cm} = \left|f(\theta)\right|^2 .$$

(See e.g. Messiah, 1961). Here k is the wave number of the incident neutron and ℓ is its orbital angular momentum state, the δ_ℓ are the phase shifts experienced by the neutron waves due to the scattering potential, and P_ℓ are Legendre polynomials whose argument is the cosine of the centre of mass scattering angle.

For n-p scattering at E_n = 22 MeV, all the phase shifts are small except δ_0 and δ_1 ; and as interactions are much weaker in odd ℓ-states than in even ℓ-states (see e.g. Enge, 1966), we have almost pure s-wave scattering, leading to an angular distribution in the centre of mass frame which is nearly isotropic.

Angular distribution measurements at E_n = 22.5 MeV, compiled by Wilson (1963) and presented in figure A1.1, support this. On the strength of this experimental result, an isotropic angular distribution in the centre of mass frame has been assumed in what follows.

Let us denote the total cross-section for s-wave scattering by σ_0. Then the differential scattering cross-section in the centre of

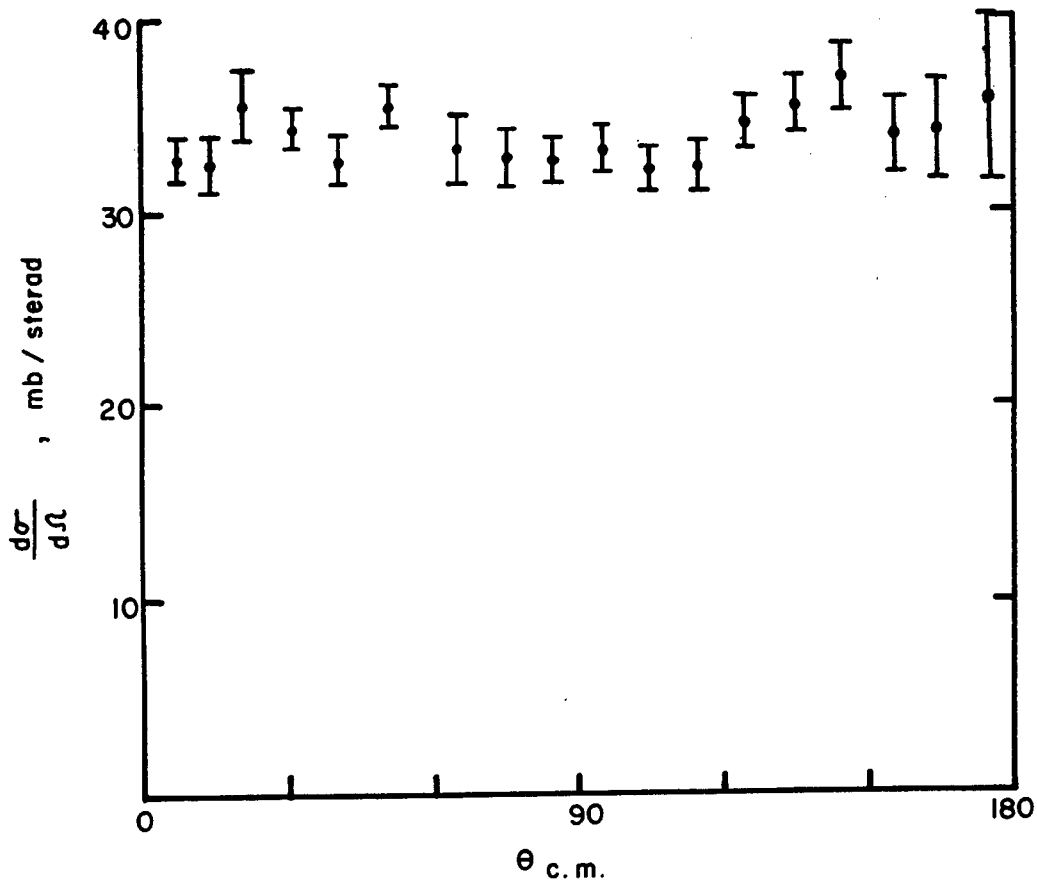

Fig. A1.1 Experimental n–p scattering angular distribution results for $E_n = 22{\cdot}5$ MeV, compiled by Wilson (1963)

mass frame is

$$d\sigma_0/d\Omega = \sigma_0/4\pi ,$$

and a (non-relativistic) transformation to laboratory coordinates yields

$$d\sigma_0/d\Omega_{lab} = (\sigma_0/\pi)\cos\theta_{lab} \qquad (0 \leq \theta_{lab} \leq \pi/2) \qquad .....(1)$$

for either the neutron or proton distribution. (The mass of a 22 MeV neutron differs from its rest mass by only 2.4%).

Taking θ_{lab} as the angle of the proton recoil relative to the incident neutron direction, kinematical considerations show that the proton energy is given by

$$E_p = E_n \cos^2\theta_{lab} \qquad .....(2)$$

where E_n is the incident neutron energy.

An examination of the reported response curves for anthracene (see figure 1.2) shows that the proton curve may be approximated by the expression

$$E_p = cL^b \qquad .....(3)$$

over the energy range 1.5 to 7.5 MeV, which includes the proton energies encountered in the spectra of Chapter 3. Here L is the light output expressed in the units of figure 1.2, and the constants have the values

$$c = 0.0136, \qquad b = 0.770 .$$

Assuming the graph to be precise, the maximum relative error incurred by this approximation is 4%.

Equations (2) and (3) together give the relation

$$\cos^2\theta_{lab} = (1/E_n)cL^b$$

which on differentiation, becomes

$$2\cos\theta_{lab}\,\sin\theta_{lab}\,d\theta_{lab} = (1/E_n)cbL^{b-1}dL. \quad .....(4)$$

(Strictly, a negative sign should appear here because $\cos\theta$ is a decreasing function while L^b is an increasing function. It is discarded). The axial symmetry of the system may be expressed by writing the element of solid angle at θ_{lab} as

$$d\Omega_{lab} = 2\pi \sin\theta_{lab}\,d\theta_{lab}\,. \quad .....(5)$$

Equations (1), (4) and (5) may be combined to show that the number of protons yielding light outputs between L and $L + \Delta L$ is proportional to

$$(d\sigma_0/d\Omega_{lab}).(d\Omega_{lab}/dL).\Delta L$$

$$= (\sigma_0/E_n)cbL^{b-1}\Delta L\,. \quad .....(6)$$

For a linear photomultiplier and amplifier combination such as that used for measurement of alpha-particle spectra, the number of counts per pulse height channel is therefore proportional to (pulse height)$^{b-1}$, where $b-1 = -0.23$ for the energy range considered.

APPENDIX 2

NEUTRON DETECTION EFFICIENCY OF A BIASED SCINTILLATION COUNTER

The purpose of this section is to determine the neutron detection efficiency, as a function of neutron energy, of the 9.3 cm x 4.0 cm NE213 liquid scintillator cell used for the neutron time-of-flight experiment, and to correct the result for the effects of the externally imposed detection threshold (in this case the bias level of the fast discriminator).

If the scintillator, of thickness x, has n effectual scattering centres per unit volume, the uncorrected detection efficiency is given by the standard result (see e.g. Enge, 1966)

$$\text{efficiency} = 1 - e^{-n\sigma x} \qquad \ldots\ldots(1)$$

where σ is the n-p scattering cross section (following Swartz and Owen (1960), who have shown that consideration of interactions with carbon makes a negligible difference to the efficiency). In the present case, x = 4cm. The number of protons per cm^3 may be calculated from the composition and density of NE213. Batchelor et al.(1961) report that the density of this liquid is 0.88gm cm^{-3}, and that the ratio of hydrogen atoms to carbon atoms is 1.21. Combining these quantities gives the result $n = 4.85 \times 10^{22} cm^{-3}$. Substitution of the values for n and x into equation (1) yields the equation

$$\text{efficiency} = 1 - e^{-0.194\sigma} \qquad \ldots\ldots(2)$$

where σ is now expressed in barns. Values of σ for various energies have been taken from the tables of Gammel (1963), and are listed in

Table A2.1. Substitution of these values into equation (2) yields the uncorrected efficiency values in column 3 of the table.

The fast bias level calibration presented in figure 2.9 shows that the cut-off introduced by the bias is not sharp, but extends over about 20 channels. Smooth curves were drawn through the points of spectra (a) and (b) of figure 2.9 and used to calculate the efficiency correction introduced by the bias level at various channels. The result is shown in figure A2.1. The straight line drawn through the points approximates the data well, and it was accepted that the bias level introduces a correction factor which is zero below channel 9, unity above channel 26, and which varies linearly as the pulse-height excess over the channel-9 pulse-height between these values. The response curves for NE213 due to Batchelor st al. (1961) indicate that the light output depends linearly on electron energy for this scintillator, and approximately linearly on proton energy over not too large ranges. In what follows it is assumed that the dependence is linear.

Let us denote the proton energy at channel 9 by E_0 and that at channel 26 by E_1 , where the subscripts refer to the efficiency correction factors introduced by the bias level.

The assumption that NE213 has a linear response to proton energy is equivalent to assuming that a recorded recoil proton spectrum will be a rectangular distribution (seen by setting $b = 1$ in equation (6) of Appendix 1). In this special case, the

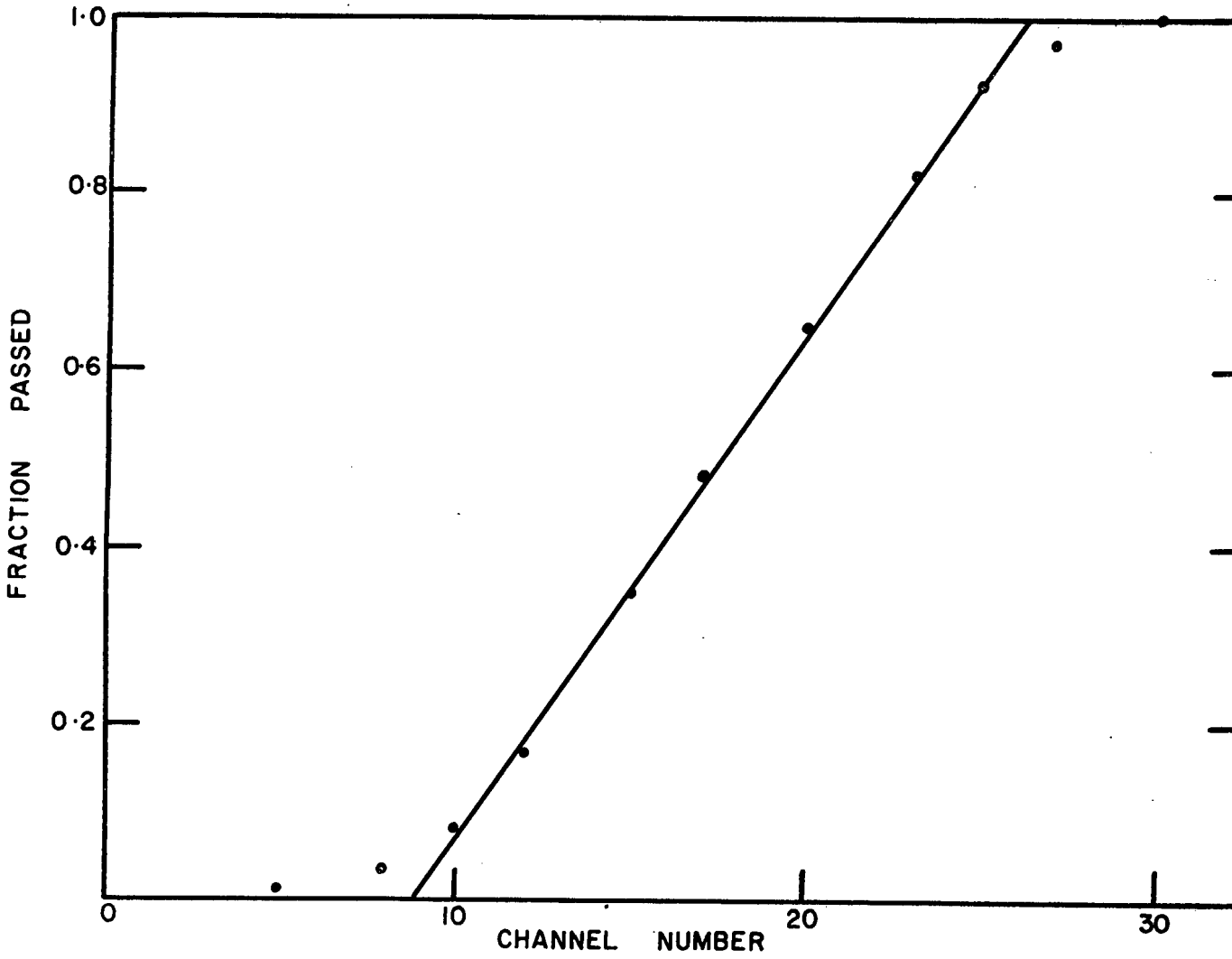

Fig. A2.1 Fraction of counts passed by fast discriminator.

TABLE A2.1

Neutron detection efficiency of NE213 cell.

E / MeV	σ_H / barn	$1-e^{-n\sigma_H x}$	F	ε
0.25	8.852	0.820	0.000	0.000
0.3	8.003	0.788	0.009	0.007
0.4	6.919	0.739	0.064	0.047
0.5	6.161	0.697	0.143	0.100
0.6	5.596	0.662	0.234	0.155
0.7	5.156	0.632	0.332	0.210
0.8	4.801	0.606	0.416	0.252
0.9	4.507	0.583	0.481	0.280
1.0	4.259	0.562	0.532	0.299
1.2	3.858	0.527	0.610	0.321
1.5	3.414	0.484	0.688	0.333
2.0	2.903	0.431	0.766	0.330
3.0	2.279	0.357	0.844	0.302
4.0	1.893	0.307	0.883	0.271
5.0	1.623	0.270	0.906	0.245
6.0	1.421	0.241	0.922	0.222
7.0	1.262	0.217	0.933	0.203
8.0	1.135	0.197	0.942	0.186
9.0	1.029	0.181	0.948	0.171
10.0	0.941	0.167	0.953	0.159
12.0	0.800	0.144	0.961	0.138
14.0	0.693	0.125	0.967	0.121
16.0	0.609	0.111	0.971	0.108
18.0	0.541	0.100	0.974	0.097
20.0	0.485	0.090	0.977	0.088
22.0	0.438	0.082	0.979	0.080

effect of the gradual cut-off on the detection efficiency may be evaluated as follows.

Suppose that in the absence of a detector bias level, a given number of monoenergetic neutrons of energy E incident at the detector give rise to a rectangular distribution having N counts per unit proton energy interval at each proton energy E_p, where $E_p \leqslant E$. Then the number of proton counts recorded is

$$\int_0^E N dE_p = NE. \qquad \ldots\ldots(3)$$

We now introduce the bias level described above. For the case $E \geqslant E_1$, the number of recorded proton events is

$$\int_{E_0}^{E_1} N (E_p - E_0)/(E_1 - E_0) \, dE_p + \int_{E_1}^{E} N dE_p$$

$$= N(E - (E_0 + E_1)/2) . \qquad \ldots\ldots(4)$$

Dividing the result (4) by (3), we obtain the detection efficiency correction factor

$$F = 1 - (E_0 + E_1)/2E \qquad (E \geqslant E_1). \qquad \ldots\ldots(5)$$

This is the standard result for a detector having a sharply-defined bias level at $(E_0 + E_1)/2$ (see e.g. Owen, 1960).

This result does not apply, however, if the incident neutron energy lies below E_1. For this case where E lies between E_0 and E_1 we see that the number of recorded proton events is

$$\int_{E_0}^{E} N\,(E_p - E_0)/(E_1 - E_0)\ dE_p$$

$$= \quad N(E - E_0)^2/2(E_1 - E_0). \qquad \text{.....(6)}$$

Dividing this result by (3) yields the detection efficiency correction factor

$$F \quad = \quad (E - E_0)^2/(2E(E_1 - E_0)) \qquad (E_0 < E < E_1) \qquad \text{.....(7)}$$

For the third possibility, namely that E is less than E_0 , we have of course

$$F \quad = \quad 0 \qquad (E \leqslant 0) \qquad \text{.....(8)}$$

Batchelor et al. (1961) have reduced their data for NE213 to the equations

$$L_e \quad = \quad E_e$$

$$L_p \quad = \quad 0.215E_p + 0.028 \qquad (E_p \leqslant 8 \text{ MeV})$$

where the electron energy E_e and the proton energy E_p are in MeV, and L_e and L_p are the corresponding pulse-heights (normalised to electron energy units). For the fast bias calibration of figures 2.9 and A2.1, these equations show that

$$E_0 \quad = \quad 0.252 \text{ MeV}, \qquad E_1 \quad = \quad 0.683 \text{ MeV}.$$

These values are used to calculate the efficiency correction F from equations (5), (7) and (8), and the results are given in column (4) of Table A2.1. The overall neutron detection efficiency ε is presented as a function of energy in column (5) of the Table, and also in figure A2.2.

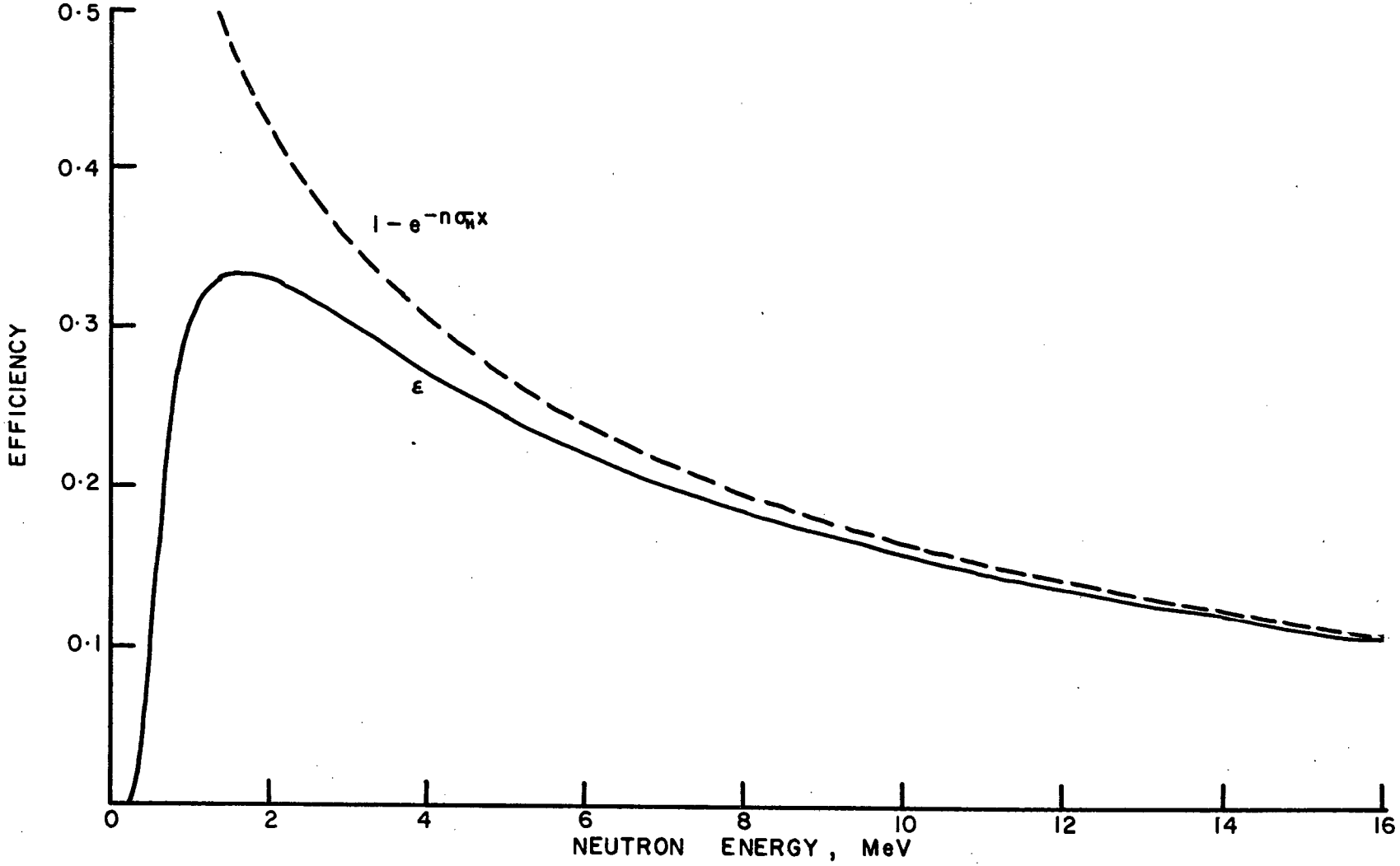

Fig. A2.2 Calculated neutron detection efficiency for NE213, 4cm. thick. Upper curve, zero bias. Lower curve, bias as used.

APPENDIX 3

DATA SMOOTHING

BY FOURTH DIFFERENCES

This local data smoothing technique is applicable to a spectrum of discrete data points $(x_i , y(x_i))$ where the x_i are equally spaced (see Lanczos, 1957). The procedure for each given data point $(x_k , y(x_k))$ is to fit the best parabola in the least squares sense to the five consecutive data points whose abscissae are $x_{k-2} , x_{k-1} , x_k , x_{k+1} , x_{k+2}$. The value of the parabola at x_k is regarded as the smoothed value of the centre point $y(x_k)$.

We wish to fit the parabola

$$y(x) = a_0 + a_1 x + a_2 x^2 \qquad \ldots\ldots(1)$$

to the five points $y(x_k)$ where $x_k = -2, -1, 0, 1, 2$. In order to minimise the mean square error

$$E = \sum_k \left[a_0 + a_1 x_k + a_2 x_k^2 - y(x_k)\right]^2$$

we require

$$\frac{\partial E}{\partial a_i} = 0, \qquad i = 0, 1, 2 .$$

This set of equations reduces to

$$\begin{aligned} 5a_0 + 10a_2 &= \sum_k y(x_k) \\ 10a_1 &= \sum_k x_k\, y(x_k) \qquad \ldots\ldots(2) \\ 10a_0 + 34a_2 &= \sum_k x_k^2\, y(x_k). \end{aligned}$$

The ordinate of the parabola $y(x)$ at $x = 0$ is given simply by the constant a_0. We therefore solve the equations (2) for a_0 to

obtain

$$a_0 = y(0) - (3/35)(y(-2) - 4y(-1) + 6y(0) - 4y(1) + y(2)) \quad \ldots\ldots(3)$$

or, in terms of the central difference operator δ,

$$a_0 = y(0) - (3/35)\delta^4 y(0). \quad \ldots\ldots(4)$$

Each value $y(x_i)$ of the original spectrum may thus be replaced by the smoothed value

$$y(x_i) - (3/35)\delta^4 y(x_i)$$

except for the last two points at either end of the spectrum.

Equation (4) gives the technique its name. For computation, however, it is sometimes simpler to use equation (3) than to compile a table of differences to the fourth order. Equation (3) forms the basis for the computer subroutine SMOOV (see Appendix 4). It should be noted that the form of equation (3) does not permit any net gain or loss of counts (y) in smoothing a large number of consecutive elements.

A modification of this technique makes it applicable to the special requirements of the analysis described in Chapter 3 for reduction of a two-parameter data matrix to component spectra.

It is required to determine the turning point of the least squares parabola described above. The turning point of the parabola of equation (1) is at

$$x_f = -(a_1/2a_2). \quad \ldots\ldots(5)$$

Equations (2) are therefore solved completely to give

$$a_1 = (1/10)(-2y(-2) - y(-1) + y(1) + 2y(2)),$$

$$a_2 = (1/14)(2y(-2) - y(-1) - 2y(0) - y(1) + 2y(2)).$$

These expressions are substituted into equation (5). The result is that the least squares parabola fitted at five consecutive abscissae $x_k = m-2, m-1, m, m+1, m+2,$ has its turning point at

$$x_t = m + x_f .$$

APPENDIX 4

COMPUTER PROGRAMS DEVELOPED FOR THE PRESENT INVESTIGATION

The three computer programs listed on the following pages were developed for the analysis of data recorded in experiments that are described in this thesis. These programs were written with the capabilities of the University's IBM 1130 computer in mind; all three have at some time also been run on an ICL 1903A computer.

The language used was Fortran IV, as modified for the 1130 machine. The flow of control for the first two programs, ALPHA and MDIFF, is fully described by the several "comment lines" interspersed among the Fortran statements. Such comments are distinguished by the appearance of the letter C in the first column, and are included purely for explanation. The third program, BACKS, is used mainly for data input and presentation, involving no major computation apart from data smoothing, already described in program MDIFF.

A4.1 PROGRAM ALPHA

```
C -- PROGRAM  ALPHA                                                              ALPHA
C -- GENERATES PROTON AND ALPHA SPECTRA FROM 2-PARAMETER PH-PSD DATA            ALPHA
C -- DEVELOPED FOR EXPERIMENTAL SERIES 4004 AT SUNI                            ALPHA
      DIMENSION TITLE(40), MAT(4100), PSD(32)                                   ALPHA 01
   14 READ (2, 100) TITLE,NRUNS,FNORM                                           ALPHA 02
  100 FORMAT (40A2 / I5, F10.0)                                                 ALPHA 03
      IF(NRUNS)99,99,10                                                         ALPHA 04
   10 WRITE (5, 200) TITLE,NRUNS,FNORM                                          ALPHA 05
  200 FORMAT (1H1, 17X, 40A2 // 26X, 'NO. OF RUNS =',      I5, '               ALPHA 06
     1 NORMALISING FACTOR = ', F10.4 ////  4X, 'PH-CHAN      E-P-CHAN         ALPHA 07
     2   P-PK-CHAN          TOTAL          ELECTRONS      TOT-LESS-EL        PRALPHA 08
     3OTONS          ALPHAS' /)                                                ALPHA 09
C -- READ  IN  MATRIX                                                           ALPHA
      DO 12 K=  1,4100                                                          ALPHA 10
   12 MAT(K) = 0                                                                ALPHA 11
      DO 60 I=1,NRUNS                                                           ALPHA012
      READ (2, 108) NFIRS, NLAST                                                ALPHA112
  108 FORMAT (2I5)                                                              ALPHA212
      READ (2, 101) (MAT(K), K=NFIRS,NLAST)                                     ALPHA312
   60 CONTINUE                                                                  ALPHA412
  101 FORMAT (7X,I6, 9I7)                                                       ALPHA 13
      MIN = 1                                                                   ALPHA 14
      DO 13 JCOL=2,128                                                          ALPHA 15
C -- SET UP PSD SPECTRUM AT PH CHANNEL JCOL AND NORMALISE                       ALPHA
      DO 11 JROW=1,32                                                           ALPHA 16
      JADDR = 128*(JROW-1) + JCOL                                               ALPHA 17
      PSD(JROW) = MAT(JADDR)                                                    ALPHA 18
   11 PSD(JROW) = FNORM * PSD(JROW)                                             ALPHA 19
C -- FIND CHANNEL OF LEAST COUNTS BETWEEN E AND P LOCI                          ALPHA
C -- LIMIT CHANGE IN 'MIN' TO ONE PER UNIT CHANGE IN JCOL                       ALPHA
      IF (MIN - 2) 42,43,43                                                     ALPHA 20
   43 IF (PSD(MIN) - PSD(MIN-1)) 42,45,45                                       ALPHA 21
   45 IF (PSD(MIN-1) - PSD(MIN+1)) 46,47,47                                     ALPHA 22
   46 MIN = MIN - 1                                                             ALPHA 23
      GO TO 50                                                                  ALPHA 24
   42 IF (PSD(MIN) - PSD(MIN+1)) 50,50,47                                       ALPHA 25
   47 MIN = MIN + 1                                                             ALPHA 26
   50 KMIN = MIN                                                                ALPHA 27
```

```
C -- FIND BEST FRACTIONAL VALUE OF MIN CHAN AND INTEGRATE TO THIS CHAN  ALPHA 27
C -- BUT FIRST ENSURE 'KMIN' IN RANGE 3 TO 30                          ALPHA
                                                                       ALPHA
      IF (KMIN - 30) 15,15,16                                          ALPHA 28
   15 IF (KMIN - 3) 18,17,17                                           ALPHA 29
   16 KMIN = 30                                                        ALPHA 30
      GO TO 17                                                         ALPHA 31
   18 KMIN = 3                                                         ALPHA 32
   17 CALL MMINT(PSD,32,KMIN,CHMIN,SUMIN,INVAL)                        ALPHA 33
      GO TO (19,2,3,4,5),INVAL                                         ALPHA 34
C -- FIND CHAN OF MAX COUNTS AFTER 'MIN', IE PROTON PEAK CHANNEL       ALPHA
   19 MIN1 = MIN + 1                                                   ALPHA 35
      MAX = MIN                                                        ALPHA 36
      DO 20 JROW = MIN1,32                                             ALPHA 37
      IF (PSD(JROW) - PSD(MAX)) 20,20,21                               ALPHA 38
   21 MAX = JROW                                                       ALPHA 39
   20 CONTINUE                                                         ALPHA 40
C -- FIND BEST FRACTIONAL VALUE OF MAX CHAN AND INTEGRATE TO THIS CHAN  ALPHA
C -- BUT FIRST ENSURE 'MAX'  IN RANGE 3 TO 30                          ALPHA
      IF (MAX - 30) 25,25,26                                           ALPHA 41
   25 IF (MAX - 3) 28,27,27                                            ALPHA 42
   26 MAX = 30                                                         ALPHA 43
      GO TO 27                                                         ALPHA 44
   28 MAX = 3                                                          ALPHA 45
   27 CALL MMINT(PSD,32,MAX,CHMAX,SUMAX,INVAL)                         ALPHA 46
      GO TO (29,2,3,4,5),INVAL                                         ALPHA 47
C -- SUBTRACT INTEGRALS TO OBTAIN HALF PROTON PEAK AND CALCULATE ALPHA COUNTS
   29 IF (JCOL - 50) 65,65,66                                          ALPHA 48
   65 CRF = 2.0                                                        ALPHA148
      GO TO 67                                                         ALPHA248
   66 C50 = JCOL - 50                                                  ALPHA348
      CRF = 2.0 + (0.010286 * C50)                                     ALPHA448
   67 PROTS = CRF * (SUMAX - SUMIN)                                    ALPHA548
      TOT = 0.0                                                        ALPHA 49
      DO 30 JROW=1,32                                                  ALPHA 50
   30 TOT = TOT + PSD(JROW)                                            ALPHA 51
      ALPHS = TOT - SUMIN - PROTS                                      ALPHA 52
C -- PRINT TOTAL, ELECTRONS, TOTAL MINUS ELECTRONS, PROTONS, ALPHAS    ALPHA
      TMINE = TOT - SUMIN                                              ALPHA 53
```

```
      WRITE (5, 202) JCOL, CHMIN, CHMAX, TOT, SUMIN, TMINE, PROTS, ALPHSALPHA 54
  202 FORMAT (1H ,  4X, I4, 2(8X,F6.2), 5(8X,F7.0))                   ALPHA 55
      GO TO 13                                                        ALPHA 56
    2 WRITE (5, 302) JCOL                                             ALPHA 57
  302 FORMAT (1H , 4X, I4, ' INPUT TO MMINT  OUTSIDE RANGE')          ALPHA 58
      GO TO 13                                                        ALPHA 59
    3 WRITE (5, 303) JCOL                                             ALPHA 60
  303 FORMAT (1H , 4X, I4, ' STRAIGHT LINE FITTED NOT PARABOLA')      ALPHA 61
      GO TO 13                                                        ALPHA 62
    4 WRITE (5, 304) JCOL                                             ALPHA 63
  304 FORMAT (1H , 4X, I4, ' TURNING POINT BELOW RANGE')              ALPHA 64
      GO TO 13                                                        ALPHA 65
    5 WRITE (5, 305) JCOL                                             ALPHA 66
  305 FORMAT (1H , 4X, I4, ' TURNING POINT ABOVE RANGE')              ALPHA 67
   13 CONTINUE                                                        ALPHA 68
C -- PLOT VISUAL REPRESENTATION OF DATA                               ALPHA
   70 G = 50.0                                                        ALPHA168
      CALL PHPSD(MAT,G,TITLE)                                         ALPHA268
C -- PREPARE FOR NEXT DATA SET                                        ALPHA
      GO TO 14                                                        ALPHA 69
   99 CALL EXIT                                                       ALPHA 70
      END                                                             ALPHA 71


      SUBROUTINE MMINT(A,IDIM,J,CHAN,SUM,INVAL)                       MMINT
      DIMENSION A(32)                                                 MMINT
      INVAL = 1                                                       MMINT
      IF (J-IDIM+2) 20,20,2                                           MMINT
   20 IF (J-3) 2,7,7                                                  MMINT
C -- LEAST SQRS PARABOLA FITTED AT 5 CHANS CENTRE J AND TURNING PT FOUNDMMINT
    7 TOP = 0.7*( A(J+1)-A(J-1) + 2.0*(A(J+2)-A(J-2)) )               MMINT
      BOT = A(J+1)+A(J-1) - 2.0*(A(J+2)-A(J)+A(J-2))                  MMINT
      IF (ABS(BOT)-0.001) 3,8,8                                       MMINT
    8 R = J                                                           MMINT
      CHAN = R + TOP/BOT                                              MMINT
      IF (CHAN-0.5) 4,15,23                                           MMINT
   23 INTPT = CHAN                                                    MMINT
      WHOLE = INTPT                                                   MMINT
```

```
      FRACT = CHAN - WHOLE                                                  MMINT
      POS = ABS(FRACT-0.5)                                                  MMINT
      IF (POS-0.001) 14,14,24                                               MMINT
   24 CHAN = CHAN + 0.02959*SIN(6.2832*FRACT)/SQRT(POS)                     MMINT
      IF (CHAN-0.5) 4,15,14                                                 MMINT
   14 IF (CHAN-32.5) 15,5,5                                                 MMINT
   15 LAST = CHAN - 0.5                                                     MMINT
      R = LAST                                                              MMINT
C -- INTEGRATE 'A' UP TO CHANNEL 'CHAN' INCLUDING FRACTIONAL PART           MMINT
      SUM = 0.0                                                             MMINT
      IF (LAST) 4,12,13                                                     MMINT
   13 DO 10 K=1,LAST                                                        MMINT
   10 SUM = SUM + A(K)                                                      MMINT
   12 SUM = SUM + (CHAN-R-0.5)*A(LAST+1)                                    MMINT
      RETURN                                                                MMINT
    2 INVAL = 2                                                             MMINT
      RETURN                                                                MMINT
    3 INVAL = 3                                                             MMINT
      RETURN                                                                MMINT
    4 INVAL = 4                                                             MMINT
      RETURN                                                                MMINT
    5 INVAL = 5                                                             MMINT
      RETURN                                                                MMINT
      END                                                                   MMINT


      SUBROUTINE PHPSD(MAT1,GDIFF,TITLE)                                    PHPSD 01
C  VISUAL PRESENTATION OF 2-PARAMETER DATA.                                 PHPSD
      DIMENSION POINT(34), REC(115), MAT1(4100), TITLE(40)                  PHPSD 02
      DATA BLANK,AXIS,POINT/' ','I','2','3','4','5','6','7','8','9','A',PHPSD 03
     1    'B','C','D','E','G','H','J','K','L','M','N','P','Q','R','S',   PHPSD 04
     2    'T','U','W','X','Y','Z','+','*','0','1'/                       PHPSD 05
C  CONVERT COUNTS-PER-STEP TO STEPS-PER-COUNT.                              PHPSD
      CONST = 1.0/GDIFF                                                     PHPSD 06
C  DIVIDE 128 ENERGY CHANNELS INTO 4 SECTIONS, ONE PLOTTED PER PAGE.        PHPSD
      DO 55 JBLOC=1,4                                                       PHPSD 07
      J32CH = 32*JBLOC                                                      PHPSD 08
      J01CH = J32CH-31                                                      PHPSD 09
```

```
      WRITE (5, 100) TITLE, JBLOC, J32CH, J01CH                          PHPSD 10
  100 FORMAT (1H1, 8X, 40A2, '      PAGE NUMBER', I2 /// 43X, 'ENERGY CHPHPSD 11
     1ANNELS', I5, '  TO', I5 ////)                                       PHPSD 12
C   SET UP ONE RECORD AT EACH OF THE 32 PSD CHANNELS.                     PHPSD
      DO 55 JROW = 1,32                                                  PHPSD 13
C   FILL RECORD WITH BLANKS AND PUT IN ONE AXIS ELEMENT PER ENERGY.       PHPSD
      DO 56 J = 1,115                                                    PHPSD 14
   56 REC(J) = BLANK                                                     PHPSD 15
      DO 57 J = 1,32                                                     PHPSD 16
      JJ = 2*J + 1                                                       PHPSD 17
   57 REC(JJ) = AXIS                                                     PHPSD 18
C   LABEL PSD AXIS IF CURRENTLY AT 10, 20 OR 30.                          PHPSD
      IF(JROW-10) 60,61,60                                               PHPSD 19
   61 REC(1) = POINT(34)                                                 PHPSD 20
      GO TO 66                                                           PHPSD 21
   60 IF(JROW-20) 62,63,62                                               PHPSD 22
   63 REC(1) = POINT(1)                                                  PHPSD 23
      GO TO 66                                                           PHPSD 24
   62 IF(JROW-30) 64,65,64                                               PHPSD 25
   65 REC(1) = POINT(2)                                                  PHPSD 26
   66 REC(2) = POINT(33)                                                 PHPSD 27
C   COMPUTE NO. OF STEPS FOR EACH ENERGY CHANNEL AT CURRENT PSD CHANNEL,  PHPSD
C   ADD 0.5 FOR ROUNDING, LIMIT STEPS TO 50, OVERWRITE WHERE NECESSARY.   PHPSD
   64 DO 50 JPH = 1,32                                                   PHPSD 28
      JCOL = 32*(JBLOC-1) + JPH                                          PHPSD 29
      JADDR = 128*(JROW-1) + JCOL                                        PHPSD 30
      COUNT = MAT1(JADDR)                                                PHPSD 31
      NSTEP = CONST * COUNT + 0.5                                        PHPSD 32
      IF(NSTEP-50) 51,51,50                                              PHPSD 33
   51 J = 67 - 2*JPH + NSTEP                                             PHPSD 34
      IF(J) 50,50,52                                                     PHPSD 35
   52 REC(J) = POINT(JPH)                                                PHPSD 36
   50 CONTINUE                                                           PHPSD 37
   55 WRITE (5, 101) REC                                                 PHPSD 38
  101 FORMAT (1H , 115A1)                                                PHPSD 39
      WRITE(5, 102)                                                      PHPSD 40
  102 FORMAT (1H1)                                                       PHPSD 41
      RETURN                                                             PHPSD 42
      END                                                                PHPSD 43
```

A4.2 PROGRAM MDIFF

```
C -- PROGRAM  MDIFF                                                          MDIFF
C -- NORMALISATION, SMOOTHING AND SUBTRACTION OF TWO 32X128 MATRICES        MDIFF
      DIMENSION  ARR(4100),           JCOL(8), OUT(16),TITLE(20)            MDIFF 00
      DEFINE FILE 1(4100, 2, U, KK)                                         MDIFF 01
C  READ CONTROL CONSTANTS FOR FIRST MATRIX.                                  MDIFF
   20 READ(2,101)TITLE,N1,FACT1,KPRIN,GDIFF                                 MDIFF 02
  101 FORMAT(20A4/2(I5,F10.0))                                              MDIFF 03
      IF (N1) 99,99,10                                                      MDIFF 04
C  READ, NORMALISE, SMOOTH FIRST MATRIX AND STORE ON DISKFILE.               MDIFF 05
   10 CALL INSMO(ARR,N1,FACT1)                                              MDIFF 06
      KK = 1                                                                MDIFF 07
      WRITE (1'KK) ARR                                                      MDIFF 08
C  READ CONTROL CONSTANTS FOR BACKGROUND MATRIX.                             MDIFF 09
      READ(2,102)N2,FACT2                                                   MDIFF 10
  102 FORMAT(I5,F10.0)                                                      MDIFF 11
      IF (N2) 99,99,19                                                      MDIFF 12
C  READ, NORMALISE, SMOOTH BACKGROUND MATRIX.                                MDIFF
   19 CALL INSMO(ARR,N2,FACT2)                                              MDIFF 13
C  RECALL SMOOTHED MATRIX FROM DISKFILE + SUBTRACT SMOOTHED BACKGROUND.      MDIFF
      DO 25 J=1,4100                                                        MDIFF 14
      KK = J                                                                MDIFF 15
      READ (1'KK) ELM                                                       MDIFF 16
   25 ARR(J) = ELM - ARR(J)                                                 MDIFF 17
      WRITE(5,103)TITLE,N1,FACT1,N2,FACT2,KPRIN,GDIFF                       MDIFF 18
  103 FORMAT(1H1,17X,20A4//12X,'NO. CHANNELS 1    FACTOR 1        NO. CHMDIFF 19
     1ANNELS 2    FACTOR 2        PRINT      DIFF. GRAPH' / 12X,          MDIFF 20
     2                         2(5X,I4,7X,F10.3,8X),I5,6X,F10.2           MDIFF 21
     3                                          ///17X,'COUNTS  AND MDIFF 22
     4 RUNNING  TOTALS  --  SUMMATION  OVER  ROW  NUMBER  FOR  EACH  COLMDIFF 23
     5UMN')                                                                 MDIFF 24
      IF(KPRIN) 15,14,15                                                    MDIFF 25
C  FOR EACH ENERGY CHAN, PRINT NET COUNTS PER PSD CHAN, AND RUN-TOTS.        MDIFF
   15 DO 7 JBLOC=1,16                                                       MDIFF 26
      DO 8 I=1,8                                                            MDIFF 27
      JCOL(I) = 8*(JBLOC-1) + I                                             MDIFF 28
    8  OUT(2*I) = 0                                                        MDIFF029
      WRITE(5,200)JCOL                                                      MDIFF 30
  200 FORMAT(1HO/1X,'COLUMN',6X,8( '(',I3,')',8X )/4X,'ROW')                MDIFF 31
      DO 7 JROW=1,32                                                        MDIFF 32
```

```
      DO 7 JROW=1,32                                                    MDIFF 32
      DO 6 I=1,8                                                        MDIFF 33
      JADDR = (JROW-1)*128 + JCOL(I)                                    MDIFF 34
       OUT(2*I-1) =  ARR(JADDR)                                         MDIFF 35
    6  OUT(2*I) =  OUT(2*I) +  OUT(2*I-1)                               MDIFF 36
    7 WRITE(5,201)JROW,( OUT(I),I=1,16)                                 MDIFF 37
  201 FORMAT(1H ,2X,I4,1X,8(F6.0,F7.0))                                 MDIFF 38
   14 IF(GDIFF) 20,20,5                                                 MDIFF 39
C  PLOT VISUAL REPRESENTATION OF NET MATRIX.                            MDIFF
    5 CALL PHP  ( ARR,GDIFF,TITLE)                                      MDIFF 40
C  PREPARE FOR NEXT DATA SET.                                           MDIFF
      GO TO 20                                                          MDIFF 41
   99 CALL EXIT                                                         MDIFF 42
      END                                                               MDIFF 43


      SUBROUTINE INSMO(ARR,NCH,FNORM)                                   INSMO
      DIMENSION ARR(4100), PSD(32), SMPSD(32)                           INSMO
C  SET PH PSD MATRIX, STORED LINEARLY, TO ZERO AND READ IN NCH POINTS.  INSMO
      DO 10 J=1,4100                                                    INSMO
   10 ARR(J) = 0.0                                                      INSMO
      READ (2, 100) (ARR(J), J=1,NCH)                                   INSMO
  100 FORMAT (7X, F6.0, 9F7.0)                                          INSMO
C  MULTIPLY BY FNORM TO NORMALISE.                                      INSMO
      DO 11 J=1,4100                                                    INSMO
   11 ARR(J) = ARR(J) * FNORM                                           INSMO
C  FOR EACH OF THE 128 ENERGY CHANNELS,                                 INSMO
      DO 12 JCOL=1,128                                                  INSMO
C  SET UP A 32 CHANNEL PSD SPECTRUM, SMOOTH, AND OVERWRITE.             INSMO
      DO 13 JROW=1,32                                                   INSMO
      JADDR = 128*(JROW-1) + JCOL                                       INSMO
   13 PSD(JROW) = ARR(JADDR)                                            INSMO
      CALL SMOOV(32,PSD,SMPSD)                                          INSMO
      DO 12 JROW=1,32                                                   INSMO
      JADDR = 128*(JROW-1) + JCOL                                       INSMO
   12 ARR(JADDR) = SMPSD(JROW)                                          INSMO
      RETURN                                                            INSMO
      END                                                               INSMO
```

```
      SUBROUTINE SMOOV (N,RAW,SMOO)                                    SMOOV
      DIMENSION RAW( 32), SMOO( 32)                                    SMOOV
C  SMOOTH 'RAW' BY 4TH DIFFERENCES, EXCEPT 2 POINTS AT EACH END.       SMOOV
      SMOO(1)  = RAW(1)                                                SMOOV
      SMOO(2)  = RAW(2)                                                SMOOV
      SMOO(N-1)= RAW(N-1)                                              SMOOV
      SMOO(N)  = RAW(N)                                                SMOOV
      K = N-2                                                          SMOOV
      DO 40 I = 3,K                                                    SMOOV
   40 SMOO(I) = RAW(I) - 0.0857143*( RAW(I-2)+ RAW(I+2)                SMOOV
     9    -4.0 *(RAW(I-1) + RAW(I+1) ) + 6.0 * RAW(I) )                SMOOV
      RETURN                                                           SMOOV
      END                                                              SMOOV


      SUBROUTINE PHP(ARR,GDIFF,TITLE)                                  PHP   01
C  VISUAL PRESENTATION OF 2-PARAMETER DATA.                            PHP
      DIMENSION POINT(34), REC(115),  ARR(4100), TITLE(20)             PHP   02
      DATA BLANK,AXIS,POINT/' ','I','2','3','4','5','6','7','8','9','A',PHP   03
     1    'B','C','D','E','G','H','J','K','L','M','N','P','Q','R','S',  PHP   04
     2    'T','U','W','X','Y','Z','+','*','0','1'/                      PHP   05
C  CONVERT COUNTS-PER-STEP TO STEPS-PER-COUNT.                          PHP
      CONST = 1.0/GDIFF                                                PHP   06
C  DIVIDE 128 ENERGY CHANNELS INTO 4 SECTIONS, ONE PLOTTED PER PAGE.    PHP
      DO 55 JBLOC=1,4                                                  PHP   07
      J32CH = 32*JBLOC                                                 PHP   08
      J01CH = J32CH-31                                                 PHP   09
      WRITE (5, 100) TITLE, JBLOC, J32CH, J01CH                        PHP   10
  100 FORMAT (1H1, 8X, 20A4, '      PAGE NUMBER', I2 /// 43X, 'ENERGY CHPHP   11
     1ANNELS', I5, '  TO', I5 ////)                                    PHP   12
C  SET UP ONE RECORD AT EACH OF THE 32 PSD CHANNELS.                   PHP
      DO 55 JROW = 1,32                                                PHP   13
C  FILL RECORD WITH BLANKS AND PUT IN ONE AXIS ELEMENT PER ENERGY.      PHP
      DO 56 J = 1,115                                                  PHP   14
   56 REC(J) = BLANK                                                   PHP   15
      DO 57 J = 1,32                                                   PHP   16
      JJ = 2*J + 1                                                     PHP   17
   57 REC(JJ) = AXIS                                                   PHP   18
```

```
C  LABEL PSD AXIS IF CURRENTLY AT 10, 20 OR 30.                          PHP
      IF(JROW-10) 60,61,60                                              PHP    19
   61 REC(1) = POINT(34)                                                PHP    20
      GO TO 66                                                          PHP    21
   60 IF(JROW-20) 62,63,62                                              PHP    22
   63 REC(1) = POINT(1)                                                 PHP    23
      GO TO 66                                                          PHP    24
   62 IF(JROW-30) 64,65,64                                              PHP    25
   65 REC(1) = POINT(2)                                                 PHP    26
   66 REC(2) = POINT(33)                                                PHP    27
C  COMPUTE NO. OF STEPS FOR EACH ENERGY CHANNEL AT CURRENT PSD CHANNEL,  PHP
C  ADD 0.5 FOR ROUNDING, LIMIT STEPS TO 50, OVERWRITE WHERE NECESSARY.   PHP
   64 DO 50 JPH = 1,32                                                  PHP    28
      JCOL = 32*(JBLOC-1) + JPH                                         PHP    29
      JADDR = 128*(JROW-1) + JCOL                                       PHP    30
      NSTEP = CONST * ARR(JADDR) + 0.5                                  PHP    31
      IF(NSTEP-50) 51,51,50                                             PHP    32
   51 J = 67 - 2*JPH + NSTEP                                            PHP    33
      IF(J) 50,50,52                                                    PHP    34
   52 REC(J) = POINT(JPH)                                               PHP    35
   50 CONTINUE                                                          PHP    36
   55 WRITE (5, 101) REC                                                PHP    37
  101 FORMAT (1H , 115A1)                                               PHP    38
      WRITE(5, 102)                                                     PHP    39
  102 FORMAT (1H1)                                                      PHP    40
      RETURN                                                            PHP    41
      END                                                               PHP    42
```

A4.3 PROGRAM BACKS

```
C -- PROGRAM  BACKS                                                              BACK01DS
C -- BACKGROUND  SMOOTHING  BY  FOURTH  DIFFERENCES                              BACK02DS
C -- ARRAYS  STORED  1 TO 512  BUT  OUTPUT  IS  0 TO 511  OR  EQUIV             BACK03DS
      DIMENSION SPECT(520),BACKG(520),SMSPE(520),SMBAC(520),SUBTR(520),         BACK04DS
     1     RTOT(5),TITLE(40),L(5)                                               BACK05DS
   69 READ (2,103) TITLE                                                        BACK06DS
  103 FORMAT (40A2)                                                             BACK07DS
      READ (2,100) NRUNS, KPRIN, DIFFG                                          BACK08DS
  100 FORMAT (2I5, F10.0)                                                       BACK09DS
      IF (NRUNS) 99,99,15                                                       BACK10DS
   15 READ (2,101) NSPEC, FSPEC, KSMSP, RAWSG, SMOSG                            BACK11DS
  101 FORMAT ( 2(I5, F10.0), F10.0)                                             BACK12DS
      READ (2,102) (SPECT(K), K=1,NSPEC)                                        BACK13DS
  102 FORMAT (7X, F6.0, 9F7.0)                                                  BACK14DS
      DO 11 I=2,NSPEC                                                           BACK15DS
   11 SPECT(I) = FSPEC  * SPECT(I)                                              BACK16DS
      IF ( KSMSP ) 13, 12, 13                                                   BACK17DS
   12 IF ( NRUNS - 1 ) 99, 28, 45                                               BACK18DS
   45 DO 16 I=2,NSPEC                                                           BACK19DS
   16 SMSPE(I) = SPECT(I)                                                       BACK20DS
      GO TO 14                                                                  BACK21DS
   13 CALL SMOOT (NSPEC, SPECT, SMSPE)                                          BACK22DS
   14 IF ( NRUNS - 1 ) 99, 28, 25                                               BACK23DS
   28 NBACK = 0                                                                 BACK24DS
      KSMBA = 0                                                                 BACK25DS
      FBACK = 0.0                                                               BACK26DS
      RAWBG = 0.0                                                               BACK27DS
      SMOBG = 0.0                                                               BACK28DS
      DO 1 I=1,NSPEC                                                            BACK29DS
      BACKG(I) = 0.0                                                            BACK30DS
    1 SUBTR(I) = 0.0                                                            BACK31DS
      GO TO 29                                                                  BACK32DS
   25 READ (2, 101) NBACK, FBACK, KSMBA, RAWBG, SMOBG                           BACK33DS
      READ (2, 102) (BACKG(K), K=1,NBACK)                                       BACK34DS
      DO 21 I=2,NBACK                                                           BACK35DS
   21 BACKG(I) = FBACK * BACKG(I)                                               BACK36DS
      IF (KSMBA) 23, 22, 23                                                     BACK37DS
   22 DO 26 I=2,NBACK                                                           BACK38DS
   26 SMBAC(I)  = BACKG(I)                                                      BACK39DS
      GO TO 27                                                                  BACK40DS
   23 CALL SMOOT (NBACK, BACKG, SMBAC)                                          BACK41DS
   27 DO 30 I=2,NSPEC                                                           BACK42DS
   30 SUBTR(I) = SMSPE(I) - SMBAC(I)                                            BACK43DS
   29 WRITE (5, 200) TITLE                                                      BACK44DS
  200 FORMAT ( 1H1, 35X, 'BACKGROUND  SMOOTHING  AND  SUBTRACTION'/////         BACK45DS
     9  15X, 40A2 )                                                            BACK46DS
      WRITE (5, 201) NRUNS, KPRIN, DIFFG, NSPEC, FSPEC,KSMSP,RAWSG,SMOSGBACK47DS
  201 FORMAT ( 1H0//66X, 'S P E C T R U M' / 20X, 'DIFFERENCE', 10X, '--BACK48DS
     9-------------------------------------'BACK49DS
     8/ '  NRUNS    PRINT        SCALE                CHANNELS    NORM FACTORBACK50DS
     7    SMOOTHING    RAW SCALE    SMOOTHED SCALE' /   I5, 4X, I5, 6X, BACK51DS
```

```
   6   F10.2, 11X, I5, 6X, F10.4, 5X, I5, 7X, F10.2, 6X, F10.2 )       BACK52DS
    WRITE (5, 202) NBACK, FBACK, KSMBA, RAWBG, SMOBG                   BACK53DS
202 FORMAT (1H0/64X,'B A C K G R O U N D'/ 40X, '--------------------BACK54DS
   9----------------------------------------'/                         BACK55DS
   8'                                          CHANNELS     NORM FACTOR BACK56DS
   7  SMOOTHING     RAW SCALE     SMOOTHED SCALE'/ 41X,                BACK57DS
   6                I5, 6X, F10.4, 5X, I5, 7X, F10.2, 6X, F10.2)       BACK58DS
    WRITE (5, 203) SPECT(1), BACKG(1)                                  BACK59DS
203 FORMAT(1H0, 'SPECTRUM    -- CHANNEL ZERO = ',  F7.0/               BACK60DS
   9           ' BACKGROUND -- CHANNEL ZERO = ',  F7.0)               BACK61DS
    IF (KPRIN) 54, 60, 54                                              BACK62DS
 54 IF (KSMSP) 70, 71, 70                                              BACK63DS
 71 DO 72 I=2,NSPEC                                                    BACK64DS
 72 SMSPE(I) = 0.0                                                     BACK65DS
 70 IF (KSMBA) 59, 74, 59                                              BACK66DS
 74 DO 75 I=2,NBACK                                                    BACK67DS
 75 SMBAC(I) = 0.0                                                     BACK68DS
 59 WRITE (5,204)                                                      BACK69DS
204 FORMAT (1H0///20X,'S P E C T R U M', 26X, 'B A C K G R O U N D'/   BACK70DS
   9' CHAN', 8X, '-------------------------------------', 8X,         BACK71DS
   8             '-------------------------------------', 10X,        BACK72DS
   7'NET     RUN'/'  NO          EXPTAL  R-TOT       SMOOTHED  R-TOT  BACK73DS
   6    ',                     'EXPTAL  R-TOT       SMOOTHED  R-TOT  BACK74DS
   5     REALS    TOT')                                               BACK75DS
    WRITE (5, 209)                                                     BACK76DS
209 FORMAT (1H ,   '----          -------------       ---------------'  BACK77DS
   3                '           -------------       ---------------'  BACK78DS
   2                '           -------------'/)                      BACK79DS
    DO 55 J= 1,5                                                       BACK80DS
 55 RTOT(J) = 0.0                                                      BACK81DS
    DO 56 I=2,NSPEC                                                    BACK82DS
    RTOT(1) = RTOT(1) + SPECT(I)                                       BACK83DS
    RTOT(2) = RTOT(2) + SMSPE(I)                                       BACK84DS
    RTOT(3) = RTOT(3) + BACKG(I)                                       BACK85DS
    RTOT(4) = RTOT(4) + SMBAC(I)                                       BACK86DS
    RTOT(5) = RTOT(5) + SUBTR(I)                                       BACK87DS
    L(1) = SPECT(I) + 0.5                                              BACK88DS
    L(2) = SMSPE(I) + 0.5                                              BACK89DS
    L(3) = BACKG(I) + 0.5                                              BACK90DS
    L(4) = SMBAC(I) + 0.5                                              BACK91DS
    L(5) = SUBTR(I) + 0.5                                              BACK92DS
    II = I-1                                                           BACK93DS
 56 WRITE (5, 205) II, L(1), RTOT(1), L(2), RTOT(2), L(3), RTOT(3),    BACK94DS
   1                   L(4), RTOT(4), L(5), RTOT(5)                    BACK95DS
205 FORMAT (1H , I4, 2(8X, I6,F7.0,7X, I6,F8.0),8X, I6, F7.0)          BACK96DS
 60 IF ( RAWSG ) 61, 61, 62                                            BACK97DS
 62 WRITE (5, 401) TITLE, RAWSG                                        BACK98DS
401 FORMAT(1H1, 15X,40A2,//25X,'GRAPH  OF  RAW  SPECTRUM  WITH  ',    BACK99DS
   9 F10.2, '  COUNTS  PER  STEP')                                     BACKA0DS
    CALL GRAPH(NSPEC,RAWSG,SPECT)                                      BACKA1DS
 61 IF ( SMOSG ) 63, 63, 64                                            BACKA2DS
```

```
 64 WRITE (5, 402) TITLE, SMOSG                                                  BACKA2DS
402 FORMAT(1H1, 15X, 40A2,//, 22X,'GRAPH  OF  SMOOTHED  SPECTRUM',              BACKA3DS
   9   '  WITH  ', F10.2, '  COUNTS  PER  STEP')                                BACKA4DS
    CALL GRAPH(NSPEC,SMOSG,SMSPE)                                              BACKA5DS
 63 IF ( RAWBG ) 65, 65, 66                                                    BACKA6DS
 66 WRITE (5, 403) TITLE, RAWBG                                                BACKA7DS
403 FORMAT (1H1, 15X, 40A2,// 24X, 'GRAPH  OF  RAW  BACKGROUND  WITH          BACKA8DS
   9', F10.2, '  COUNTS  PER  STEP')                                           BACKA9DS
    CALL GRAPH(NBACK,RAWBG,BACKG)                                              BACKB0DS
 65 IF ( SMOBG ) 67, 67, 68                                                    BACKB1DS
 68 WRITE (5, 404) TITLE, SMOBG                                                BACKB2DS
404 FORMAT (1H1, 15X, 40A2,//,22X, 'GRAPH  OF  SMOOTHED  BACKGROUND  WBACKB3DS
   9ITH  ', F10.2, '  COUNTS  PER  STEP')                                      BACKB4DS
    CALL GRAPH(NBACK,SMOBG,SMBAC)                                              BACKB5DS
 67 IF ( DIFFG) 69, 69, 79                                                     BACKB6DS
 79 WRITE (5, 405) TITLE, DIFFG                                                BACKB7DS
405 FORMAT (1H1, 15X, 40A2,//,  5X, 'GRAPH  OF  SPECTRUM  MINUS  BACKGBACKB8DS
   9ROUND  WITH  SMOOTHING  AS  REQUESTED.  SCALE  ', F10.2, '  COUNTSBACKB9DS
   8  PER  STEP')                                                             BACKC0DS
    CALL GRAPH(NSPEC,DIFFG,SUBTR)                                              BACKC1DS
    GO TO 69                                                                   BACKC2DS
 99 CALL EXIT                                                                  BACKC3DS
    END                                                                        BACKC4DS
    SUBROUTINE SMOOT (N,RAW,SMOO)                                              BACKC5DS
    DIMENSION RAW(520), SMOO(520)                                              BACKS1DS
    SMOO(1)   = RAW(1)                                                         BACKS2DS
    SMOO(2)   = RAW(2)                                                         BACKS3DS
    SMOO(3)   = RAW(3)                                                         BACKS4DS
    SMOO(N-1)= RAW(N-1)                                                        BACKS5DS
    SMOO(N)   = RAW(N)                                                         BACKS6DS
    K = N-2                                                                    BACKS7DS
    DO 40 I = 4,K                                                              BACKS8DS
 40 SMOO(I) = RAW(I) - 0.0857143*( RAW(I-2)+ RAW(I+2)                          BACKS9DS
   9     -4.0 *(RAW(I-1) + RAW(I+1) ) + 6.0 * RAW(I) )                        BACKT0DS
    RETURN                                                                     BACKT1DS
    END                                                                        BACKT2DS
    SUBROUTINE GRAPH(N,SCALE,POINT)                                            BACKT3DS
    REAL LINE(111)                                                             BACKG1DS
    DIMENSION POINT(520)                                                       BACKG2DS
    DATA BLANK,AXIS,DOT/' ','I','X'/                                           BACKG3DS
    DO 80 J=1,111                                                              BACKG4DS
 80 LINE(J)=BLANK                                                              BACKG5DS
    CONST = 1.0/SCALE                                                          BACKG6DS
    WRITE (5, 302)                                                             BACKG7DS
302 FORMAT(1HO//3X,'-10',9X,                                                   BACKG8DS
   1           '0',8X,'10',8X,'20',8X,'30',8X,'40',8X,'50',8X,                 BACKG9DS
   2'60',8X,'70',8X,'80',8X,'90',7X,'100')                                     BACKH0DS
    LAB10 = 0                                                                  BACKH1DS
    DO 12 LOOP=1,N                                                             BACKH2DS
    LABEL = LOOP-1                                                             BACKH3DS
    DO 6 I=1,12                                                                BACKH4DS
                                                                               BACKH5DS
```

```
      DATA BLANK,AXIS,DOT/' ','I','X'/                                  BACKG4DS
      DO 80 J=1,111                                                     BACKG5DS
   80 LINE(J)=BLANK                                                     BACKG6DS
      CONST = 1.0/SCALE                                                 BACKG7DS
      WRITE (5, 302)                                                    BACKG8DS
  302 FORMAT(1HO//3X,'-10',9X,                                          BACKG9DS
     1           '0',8X,'10',8X,'20',8X,'30',8X,'40',8X,'50',8X,        BACKH0DS
     2'60',8X,'70',8X,'80',8X,'90',7X,'100')                            BACKH1DS
      LAB10 = 0                                                         BACKH2DS
      DO 12 LOOP=1,N                                                    BACKH3DS
      LABEL = LOOP-1                                                    BACKH4DS
      DO 6 I=1,12                                                       BACKH5DS
      J = 10*I-9                                                        BACKH6DS
    6 LINE(J) = AXIS                                                    BACKH7DS
      J = CONST * POINT(LOOP ) +11.5                                    BACKH8DS
      IF (J-1) 2, 3, 3                                                  BACKH9DS
    2 J=1                                                               BACKJ0DS
    3 IF (J-111) 4, 4, 5                                                BACKJ1DS
    5 J = 111                                                           BACKJ2DS
    4 LINE(J) = DOT                                                     BACKJ3DS
      IF (LABEL - LAB10) 10, 11, 10                                     BACKJ4DS
   11 WRITE (5, 303) LABEL, LINE                                        BACKJ5DS
  303 FORMAT (1H ,I4,111A1)                                             BACKJ6DS
      LAB10 = LAB10 +10                                                 BACKJ7DS
      GO TO 12                                                          BACKJ8DS
   10 WRITE (5, 304) LINE                                               BACKJ9DS
  304 FORMAT (1H ,4X,111A1)                                             BACKK0DS
   12 LINE(J) = BLANK                                                   BACKK1DS
      RETURN                                                            BACKK2DS
      END                                                               BACKK3DS
```

ACKNOWLEDGEMENTS

I wish to express my sincere appreciation to all those who have assisted in bringing this thesis to completion. I am especially indebted to the following:

My supervisor, Professor F.D. Brooks of the University of Cape Town, for his guidance, help and encouragement;

Dr W.R. McMurray of the Southern Universities Nuclear Institute, for the interest he has shown in this project;

The staff of S.U.N.I. for their co-operation and assistance;

My colleagues at U.C.T., for their assistance during the running of the experiments, and at the time of developing the computer programs;

Mrs Ensor of the U.C.T. Computer Centre, for much assistance in punching data onto computer cards;

My wife, Lesley, for careful preparation of the diagrams and typing of the stencils, and Miss A. Blane, who assisted with the typing.

LIST OF REFERENCES

Ajzenberg-Selove, F., Lauritsen, T., 1968. Nuc. Phys. A114, 1.

Bame, S. J., Perry, J. E., 1957. Phys. Rev. 107, 1616.

Barjon, R., Flamant, Y., Perchereau, J., Rode, A., 1962. Nuc. Phys. 36, 247.

Batchelor, R., Gilboy, W. B., Purnell, A. D., Towle, J. H., 1960. Nuc. Instr. and Meth. 8, 146.

Batchelor, R., Gilboy, W. B., Parker, J. B., Towle, J. H., 1961. Nuc. Instr. and Meth. 13 , 70.

Birks, J. B., 1964. The Theory and Practice of Scintillation Counting (Pergamon Press).

BNL 400, 1970. Angular Distributions in Neutron-Induced Reactions Volume 1, Z=1 to 20 (Brookhaven National Laboratory).

Brooks, F. D., 1956. Progress in Nuclear Physics, ed. O. R. Frisch (Pergamon Press) 5 , 284.

Brooks, F. D., 1959. Nuc. Instr. and Meth. 4 , 151.

Brooks, F. D., Pringle, R. W., Funt, B. L., 1960. I.R.E. Trans. Nucl. Sci. NS-7 , 35.

de Vries, L. J., Udo, F., 1961. Nuc. Instr. and Meth. 13 , 153.

Egelstaff, P. A., Rae, E. R., 1964. Automatic Acquisition and Reduction of Nuclear Data, eds. K. H. Beckurts, W. Gläser, G. Kruger (Gesellschaft für Kernforschung m.b.H. Karlsruhe) pp. 83-95.

Enge, H. A., 1966. Introduction to Nuclear Physics (Addison - Wesley).

Frye, G. M., Rosen, L., Stewart, L., 1955. Phys. Rev. 99 , 1375.

Gammel, J. L., 1963. Fast Neutron Physics, eds. J. B. Marion, J. L. Fowler (Interscience Publishers) pp. 2185-2226.

Goldberg, M. D., 1963. Progress in Fast Neutron Physics, eds. Phillips, G. C., Marion, J. B., Risser, J. R. (Univ. of Chicago Press) pp. 9-12.

Gooding, T. J., Pugh, H. G., 1960. Nuc. Instr. and Meth. 7 , 189.

Grin, G. A., Vaucher, B., Joseph, C., Alder, J. C., Loude, J. F., 1965. Helv. Phys. Acta 38 , 368.

Grin, G. A., Joseph, C., Vaucher, B. Alder, J. C., Loude, J. F., Henchoz, A., 1965. Helv. Phys. Acta 38 , 666.

Grin, G. A., Joseph, C., Alder, J. C., Vaucher, B., Loude, J. F., 1966. Helv. Phys. Acta 39 , 214.

Grin, G. A., Vaucher, B., Alder, J. C., Joseph, C., 1969. Helv. Phys. Acta 42 , 990.

Henchoz, A., Joseph, C. 1965. Helv. Phys. Acta 38 , 663.

Jessen, P., Bormann, M., Dreyer, F., Neuert, H., 1966. Nuclear Data A1 , 107.

Johnson, F. A., 1963. Canadian J. Phys. 41 , 793.

Jones, D. T. L., 1967. MSc Thesis, University of Cape Town (unpublished).

Joseph, C., Grin, G. A., Alder, J. C., Vaucher, B., 1967. Helv. Phys. Acta 40 , 693.

Kunz, W., Schintlmeister, J., 1967. Nuclear Tables Part II. (Pergamon).

Lanczos, C., 1957. Applied Analysis (Pitman).

Loude, J. F., Perroud, J. P., Sellem, C., 1969. Helv. Phys. Acta 42 , 905.

Messiah, A., 1961. Quantum Mechanics, Volume 1 (Wiley and Sons).

Notarrigo, S., Porto, F., Rubbino, A., Sambataro, S., 1969. Nuc. Phys. A125 , 28.

Owen, R. B., 1958. I.R.E. Trans Nuc. Sci. NS-5 , 198.

Peelle, R. W., 1957. Phys. Rev. 105 , 1311.

Perkin, J. L., 1951. Phys. Rev. 81 , 892.

Swartz, C. D., Owen, G. E., 1960. Fast Neutron Physics Part 1, eds. J. B. Marion, J. L. Fowler (Interscience Publishers).

Tsukada, K., Kikuchi, S., 1962. Nuc. Instr. and Meth. 17 , 286.

Wilson, R., 1963. The Nucleon-Nucleon Interaction (Interscience Publishers).